Bedford Institute of Oceanography
l'institut oceanographiqué de Bedford
Dartmouth/Nova Scotia/Canada

Design and Installation of the Atlantic Oceanographic Laboratory Stable Platform

R. G. Mills

Report Series/BI-R-72-4/July 1972

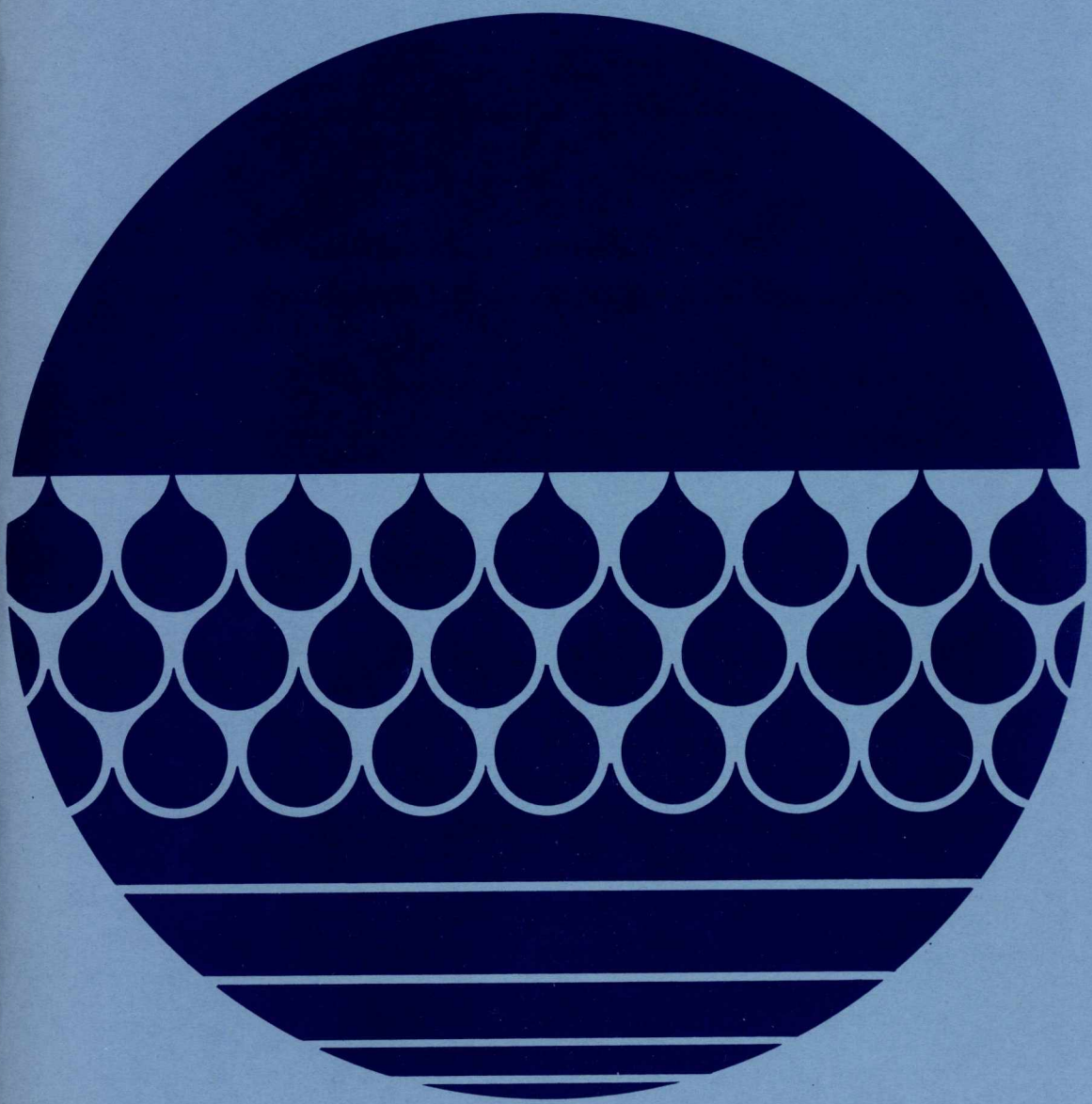

The Bedford Institute of Oceanography is a Government of Canada establishment whose staff undertake scientific research and surveys in the marine environment. It consists of three main units, (1) the Atlantic Oceanographic Laboratory, which is part of the Marine Sciences Branch of the Department of the Environment, (2) the Marine Ecology Laboratory of the Fisheries Research Board of Canada, also of the Department of the Environment, and (3) the Atlantic Geoscience Centre of the Department of Energy, Mines and Resources.

Cover Design/Keith Clarridge

BEDFORD INSTITUTE OF OCEANOGRAPHY

Dartmouth, Nova Scotia
Canada

DESIGN AND INSTALLATION

OF THE

ATLANTIC OCEANOGRAPHIC LABORATORY

STABLE PLATFORM

by

R.G. Mills

Atlantic Oceanographic Laboratory
Marine Sciences Directorate
Department of the Environment

JULY 1972 REPORT SERIES BI-R-72-4

ABSTRACT

The Atlantic Oceanographic Laboratory, Bedford Institute of Oceanography, has developed a small offshore structure for air-sea interaction studies and oceanographic research. The three-legged diagonally cross-braced structure weighs 25 tons, is 65 metres in length and is a 2.45-metre equilateral triangle in cross section. The structure sits on the sea bed and is held in position by a system of guy wires. It was moored in 57 metres of water off the coast of Nova Scotia and although it failed to survive a severe storm it did withstand 8-metre seas for an extended period.

It is relatively inexpensive to construct and install and yet provides an all-weather instrument platform stable enough for air-sea interaction studies while being small enough to have a negligible effect on the parameters being observed.

This report reviews the design, installation and performance of the structure and the instrumentation developed to monitor its performance.

LIST OF CONTENTS

LIST OF FIGURES

LIST OF TABLES

1. INTRODUCTION

In recent years, the exchanges of energy between air and sea have received increasing attention from meteorologists and oceanographers. The importance of this work can only be realized when one considers the far-reaching effects of these exchanges. The action of the wind on the ocean surface causes waves and wind-driven circulation. The evaporation of water from the oceans and subsequent precipitation is the primary source of the world's fresh water. The transfer of the latent heat of vaporization between the oceans and the atmosphere is the driving force behind global wind circulation, and the principal source of energy for weather of all kinds. This continuing transfer between the atmosphere and the oceans is how nature purifies and distributes the two essential requirements for the support of life, air and water.

The mechanisms of these exchanges have been under study by the air-sea interaction group at the Atlantic Oceanographic Laboratory, Bedford Institute of Oceanography, since the early sixties and a continuing problem has been the development of an instrument capable of measuring small fluctuations in the mean wind velocity. A three-component wind thrust anemometer to provide this data was conceived by L.A.E. Doe (1963) and the Mark VI anemometer (Smith, 1969) presently used by AOL has developed from this concept. This instrument is extremely sensitive to accelerations and requires a stable support to provide meaningful data, and therefore the use of free-floating buoys or conventional vessels is not feasible. The mast should also be slender to avoid disturbing the air flow and the phenomena being observed, and this requirement severely limits the usefulness of drilling rigs or structures of similar size. To provide a suitable offshore mounting platform for the thrust anemometer the AOL Stable Platform has been developed over a number of years. Figure 1 is a photograph of the most recent platform (the Mark III) installed at the entrance to Halifax Harbour.

2. DEVELOPMENT

The development of an offshore structure suitable for air-sea interaction research began at AOL in 1964 with the mooring of a taut wire buoy, 25 metres in length, off Aruba. This was probably the first floating structure to use multiple mooring lines (9) in an attempt to achieve a stable structure suitable for air-sea interaction research (Doe and Brooke, 1965). In 1965 the buoy was modified to a bottom-resting configuration and moored off Prince Edward Island. Reverting to the taut wire configuration, but with two mooring lines - one to moor the buoy and the second to prevent rotation - the buoy was moored in the Great Lakes and used by the Department of Transport and AOL in 1966. Based on the prototype, a new structure 38 metres in length was designed under the direction of J. Brooke of AOL and three were constructed by DOT in Cornwall, Ontario. Of these two were used by DOT as meteorological stations in the Great Lakes and the other by AOL for air-sea interaction research. The AOL version was known as the Mark I Stable Platform and was a floating structure held in position using multiple mooring lines (13) and thirteen 25-ton concrete anchors (Smith, 1969). The Mark I platform resembled the taut wire buoy developed at the Great Lakes Institute (Deane, 1963) and that developed for Woods Hole Oceanographic Institution (Pearlman, 1964). It was moored off Chebucto Head near the approaches to Halifax Harbour

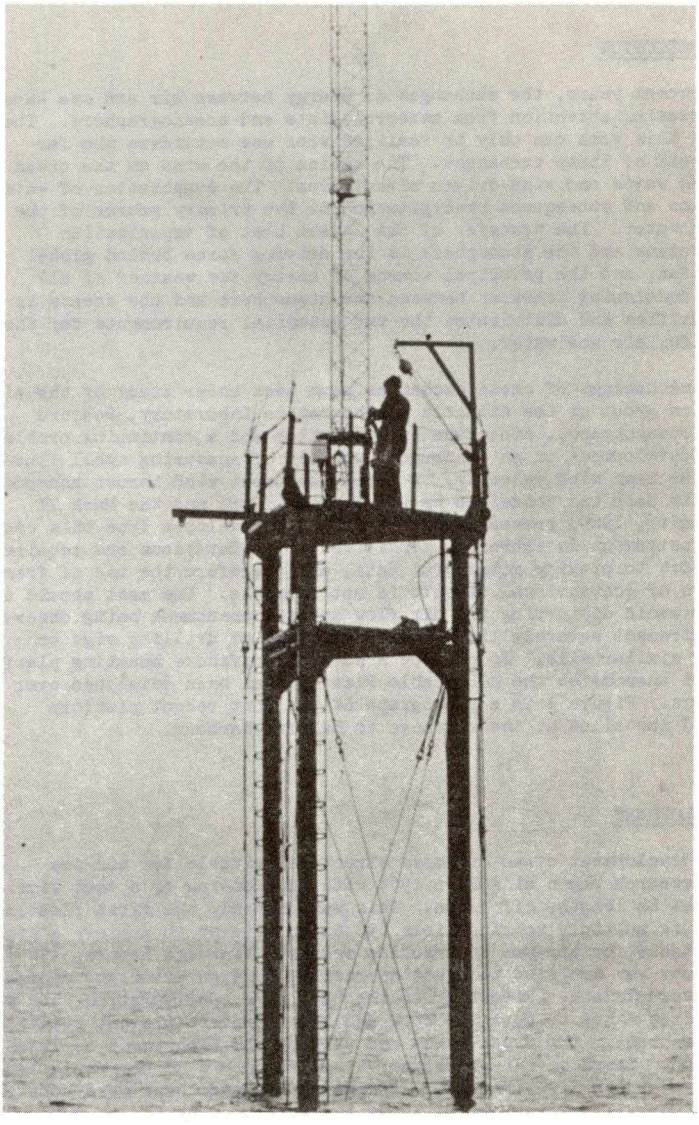

FIGURE 1: Installed Stable Platform

(44°27'33"N, 63°31'45"W) and was a successful installation remaining in position from October 1967 to October 1968 when changing scientific requirements and complaints by local fishermen led to its being removed. A disadvantage of the Mark I was that it required the accurate placement of 13 anchors, an extremely difficult undertaking under open sea conditions. More important is that a taut buoy system, even with multiple mooring wires, is more prone to vertical and rotary motion than a bottom-mounted structure. While it is possible to resolve errors in the thrust anemometer data caused by the pitch of a bottom-mounted structure, the cross coupling of pitch, heave and rotary motion experienced with a taut buoy system is extremely difficult to correct for satisfactorily.

To overcome the disadvantages of the Mark I, the Mark II was a bottom-mounted structure held in position by three equally-spaced mooring wires each attached to a 5-ton ship anchor. It was 64 metres in length and similar in principle to the bottom-mounted structure developed at the Great Lakes Institute, University of Toronto (Dean, 1963). The design and installation were conducted for AOL by Gibb, Alberry, Pullerits and Dickson (1969), Consulting Engineers, Halifax, Nova Scotia. To extend the maximum mean wind speed under which air-sea interaction observations could be made from the 10 to 15 m/s range available at the Mark I location off Chebucto Head, the Mark II was installed at the entrance to Halifax Harbour (44°29'26"N, 63°23'31"W) where 20-25 m/s wind speeds were available. It was installed in April 1969, and after numerous problems failed in December 1969 although it did demonstrate that meaningful data (Smith, 1970) could be obtained from a bottom-mounted structure. The cause of failure was anchor movement resulting from the wrong choice of anchor. A conventional stockless ship anchor of the type used relies on weight and some degree of hooking for a holding power of approximately three times its weight providing the pull on the anchor is horizontal. Unfortunately, this requirement was not compatible with the use of wire mooring rope as its low weight resulted in the direction of pull on the anchor being in line with the mooring wire attachment point on the structure (22 degrees to horizontal). The use of chain mooring lines would have ensured that the pull was horizontal but the resulting reduction in stiffness due to the increased catenary would have allowed the structure too great a freedom of movement. Other shortcomings of the 1969 installation which became evident during its time *in situ* were that waves higher than 8 metres occurring at high tide subjected the work platform to wave action and a substantial area was therefore presented to the waves at a point where their action was most severe, the crest. This area was further increased by the addition of the electronic equipment and the battery packs used to power it. To reduce the effects of wave action the upper 9 metres of the structure had no diagonal cross bracing and the resulting loss in strength was illustrated by failure of the joints. Also, with three mooring wires at 120 degrees, the structure had insufficient resistance to twisting.

The 1970 installation of the Mark III structure, as described in this publication, attempted to overcome the deficiencies of the Mark II while retaining the same bottom-mounted configuration. Concrete anchors were used to provide holding power independent of both bottom conditions and the direction of pull of the mooring lines; and the number of mooring wires was increased to four to reduce any twisting action. When a four-point mooring system is used on a three-legged structure, the fourth attachment point is normally introduced between two of the legs permitting the use of four wires

at 90 degrees arranged such that opposing wires are directly in line. As the introduction of a fourth anchor point between two of the legs was not compatible with a streamlined structure near the water level the Mark III mooring system was a compromise with 60- and 120-degree included angles as shown in Figure 9. This configuration permitted the introduction of the fourth mooring wire without the introduction of an attachment point between the legs. The opposing wires were also directly in line and therefore prevented twisting. The configuration had a preferred direction as the mooring wires were not equally spaced but this was not detrimental as general directions of the worst storms were known and the platform was orientated accordingly. The overall height was increased to minimize the chance of the work platform being subjected to wave action, and the area of the platform was reduced. The size of the instrumentation package installed on the platform was also minimized and provision was made to power the system from a battery pack installed on the sea bed. In October 1970 the structure was installed in the same position as the Mark II (Fig. 2) as experience had shown that the bottom was sand and gravel with a conservative value of bearing strength of 11 ton/m^2 and that scouring around the base was not a problem.

3. DESCRIPTION

The configuration of the Mark III structure is shown in Figures 3 and 4 and additional details are contained in the working drawings E-B-19-1, E-B-19-2 included with the report. The structure was 65 metres in length, a 2.4-metre equilateral triangle in cross section, and was constructed from 15 sections which were bolted together. It was made of steel and as the basic structure was in existence no consideration was given to the use of alternative materials, but it is probable that steel was favourable from both a practical and economic standpoint. Corrosion protection was provided by a 3-mil thick coating of inorganic zinc. Prior to application of the inorganic zinc it was sandblasted to Commercial Blast Standard No. 6 and the inorganic zinc applied immediately to prevent humid conditions starting the corrosion process. The complete structure was then coated with an aluminum barrier coat followed by an anti-fouling paint below the water level and two coats of vinyl enamel above the water level. The four tank sections each had six zinc anodes to provide additional protection against corrosion. The tank sections were in two groups of two and provided a total of 36 tons displacement giving a reserve buoyancy of 12.6 tons over the structure weight of 23.4 tons. The piping configuration (Fig. 5) was the same for all tanks and permitted independent flooding and pumping of each tank. The structure was trimmed by controlled flooding of the lower tanks, but this was an extremely critical operation and practice was required to consistently trim to a particular angle. In the moored position the upper tanks remained unflooded to provide sufficient restoring force to keep the work platform above sea level in the event of a mooring system failure. Experience showed this to be an essential requirement. For maximum restoring force, the upper tanks should be as near the water level as possible; but as this was not compatible with minimizing the wave force on the tanks, the final position was a compromise. To recover the structure, the lower tanks were pumped dry using a 5 m^3/min portable air compressor installed on a small fishing boat. For this operation two hundred feet of flexible 2.5 cm diameter high pressure air line were used to connect the compressor to

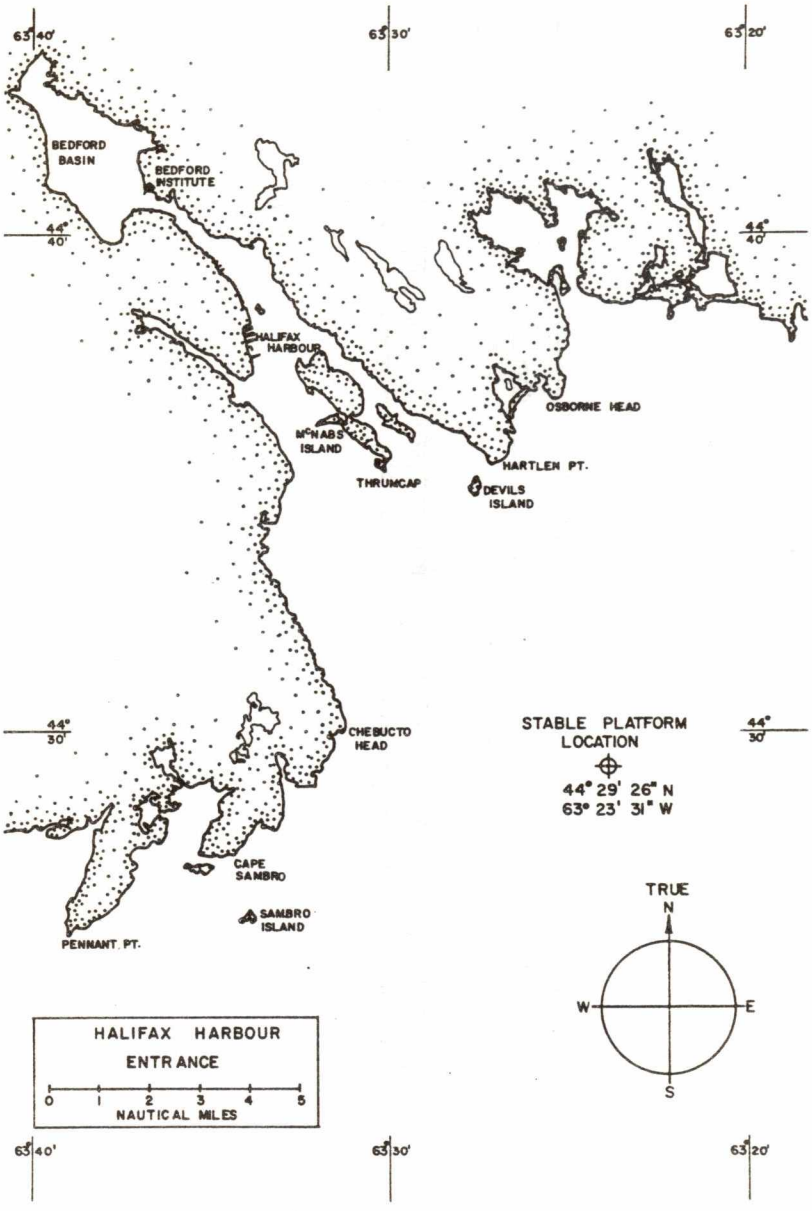

FIGURE 2: Mark III Location

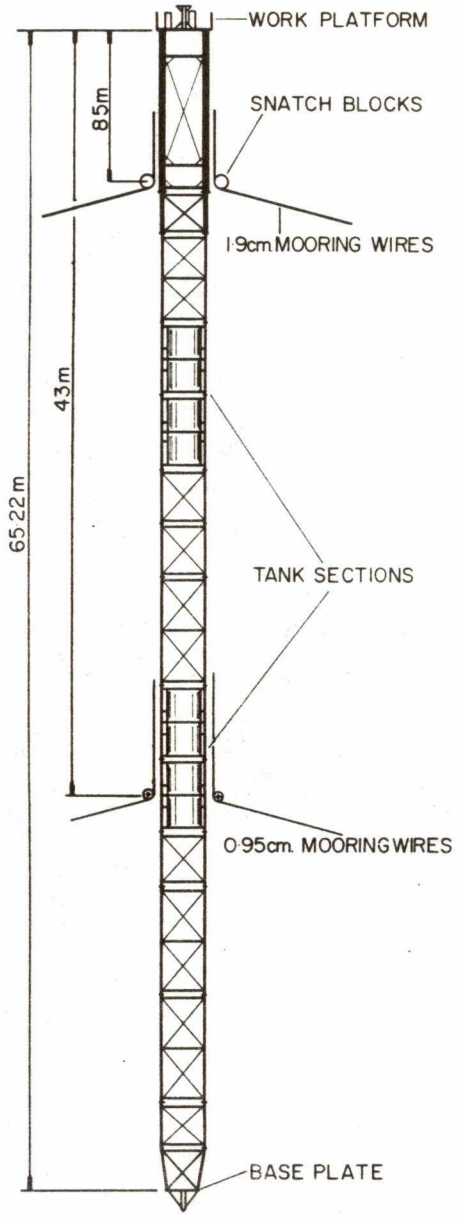

FIGURE 3: Configuration of Structure

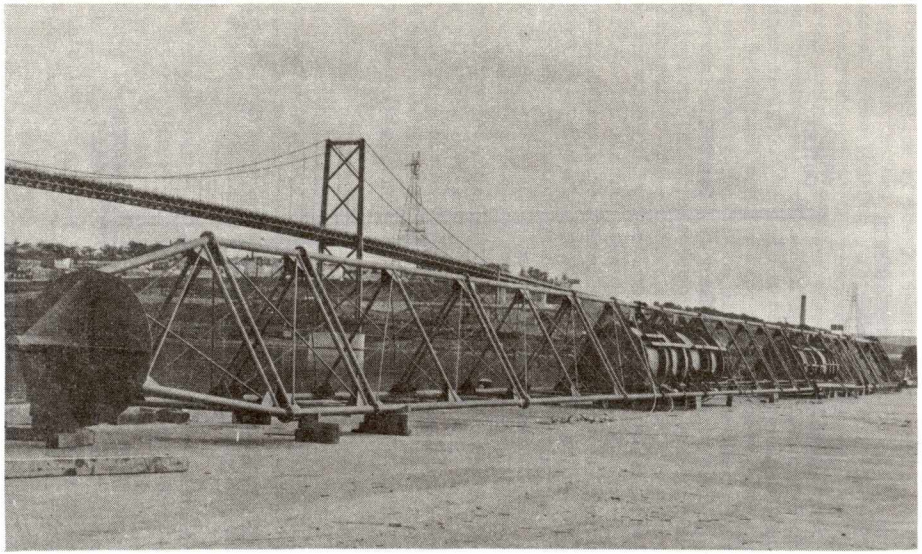

FIGURE 4: Structure on Bedford Institute Wharf

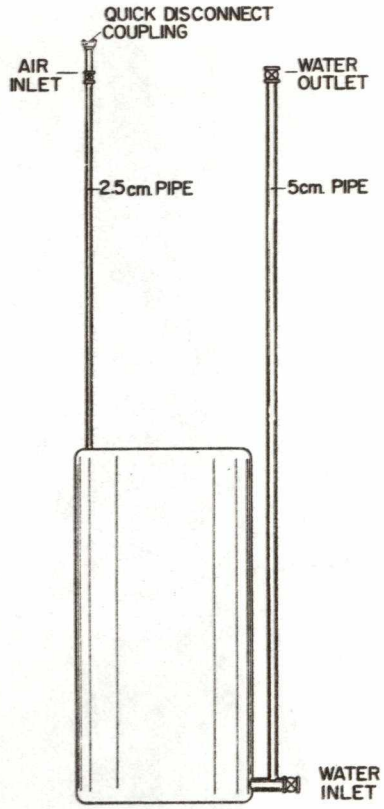

FIGURE 5: Piping Configuration

the tank valves and quick disconnect couplings were used to facilitate easy attachment and removal. As the tank fittings terminated 6 metres below the water level, divers were required for this operation.

The construction of the 9.15-metre top section differed from that of the standard sections in that it utilized 0.2-metre pipe as main members and had less diagonal cross bracing. This relatively open configuration provided a minimum of interference to the phenomena being observed and the reduction in the number of structural members also reduced the effect of ice loading. Diagonal cross bracing was omitted in 1969 but failure of the joints led to its introduction in 1970. To tension the mooring wires during the mooring operation four 5-ton hand winches were mounted on the work platform. These winches were subsequently removed to minimize the area subject to wave action; to increase the available work area, and to protect the winches from corrosion. To replace the winches every time the mooring wires needed tensioning was impractical and a portable chain hoist was substituted for this purpose. The arrangement for tensioning the guy wires with a chain hoist is shown in Figure 6. To simplify the installation of the structure two temporary work platforms were installed on the top section (Fig. 7). The first 1.5 metres below the work platform provided access to the turnbuckles and mooring wire anchor plates, and the second consisting of three 0.25-metre wide boards 8 metres below the work platform access to the 1.9 cm mooring wire swivel snatch blocks. A 6-metre aluminum radio mast was mounted in the centre of the work platform and guyed at the 3-metre and 10-metre levels. The accelerometer package, aerovane anemometer, transmit and receive antenna and navigational warning light were mounted on the radio mast and the electronics canister used for controlling the operation of the scientific instruments was mounted at its base (Fig. 8).

The purpose of the lowest section was to support the weight of the structure, prevent lateral movement and minimize twisting. Resistance to lateral movement and twisting was provided by four flukes that penetrated the sea bed, and the weight of the structure was supported by a load-bearing plate 2.4 metres^2 in area. In the moored position, with the upper tanks buoyant, the downward load was 5.4 tons giving a bearing load of 2.25 ton/m^2.

The structure was held in position by mooring wires and concrete clump anchors as shown in Figures 9 and 10. The main mooring wires were 1.9 cm diameter, 6x24 construction, wire rope core, galvanized improved plow steel with a breaking strength of 16.8 tons. Each concrete anchor weighed 12 tons in air and the 82-metre connecting chain between the anchors, 2 tons. The main 1.9 cm mooring wires passed through swivel snatch blocks 8.5 metres below the work platform and terminated in turnbuckles at the platform. Swivel snatch blocks were used to accommodate possible errors in the anchor layout or positioning of the structure. The turnbuckles were 3.2 cm diameter and 0.61 metre take-up with jaw and jaw ends and provided a fine adjustment for the wire tension. They were instrumented with strain gauges and displayed the wire tension on electrical meters on the work platform. The working range of the turnbuckle instrumentation was 0-9 tons. The 0.95 cm diameter galvanized steel wires used during the installation passed through swivel snatch blocks 49 metres below the work platform and terminated 1.5 metres below the platform where they were wire-clipped to gusset plates.

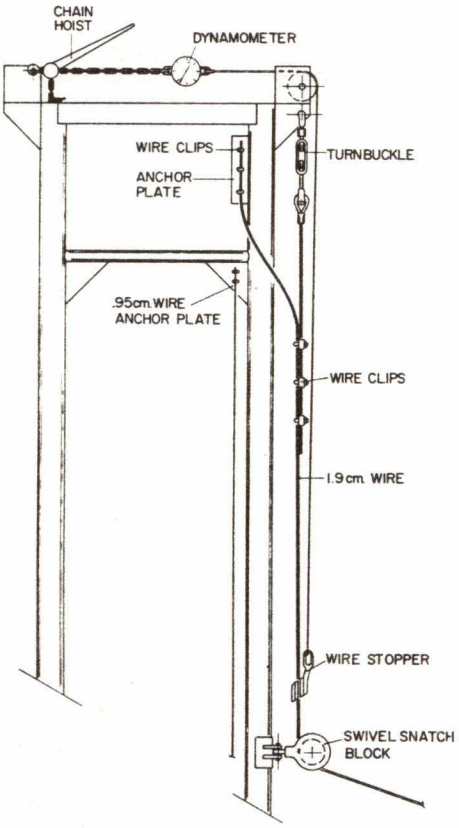

FIGURE 6: Chain Hoist Tensioning

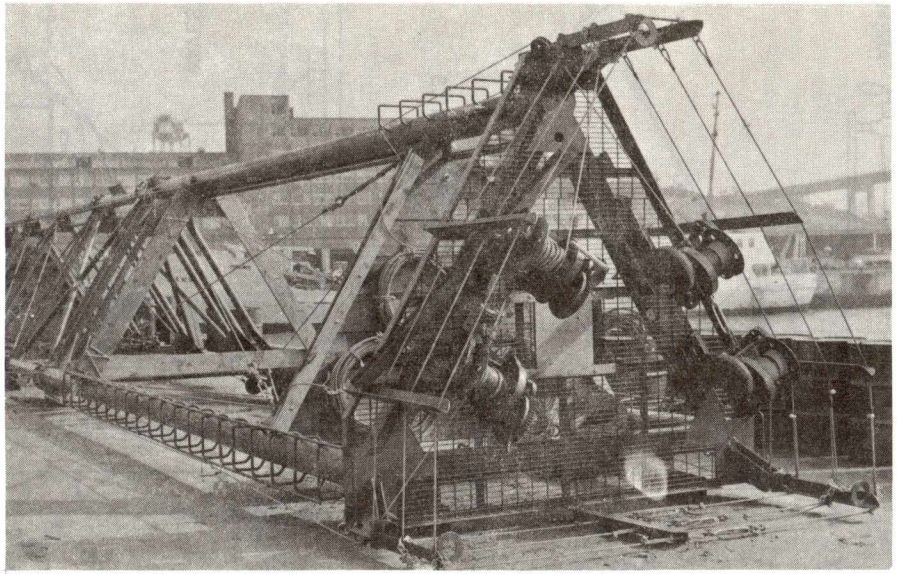

FIGURE 7: Temporary Work Platforms

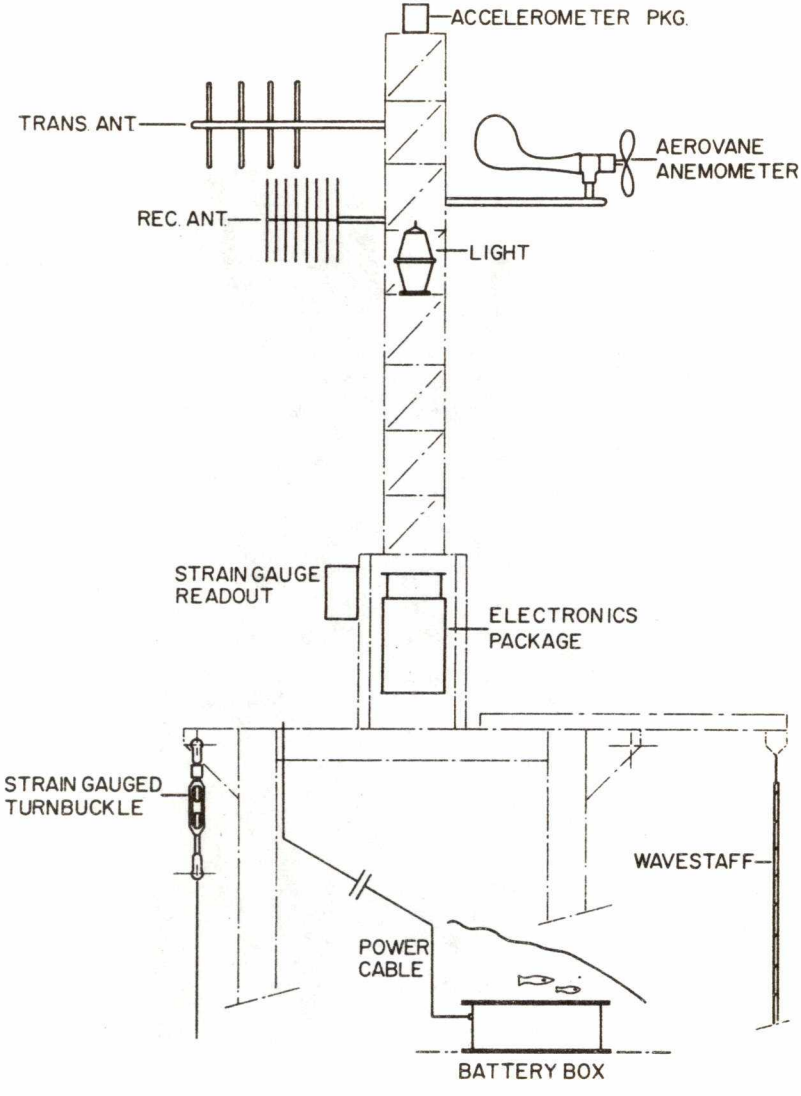

FIGURE 8: Instrumentation

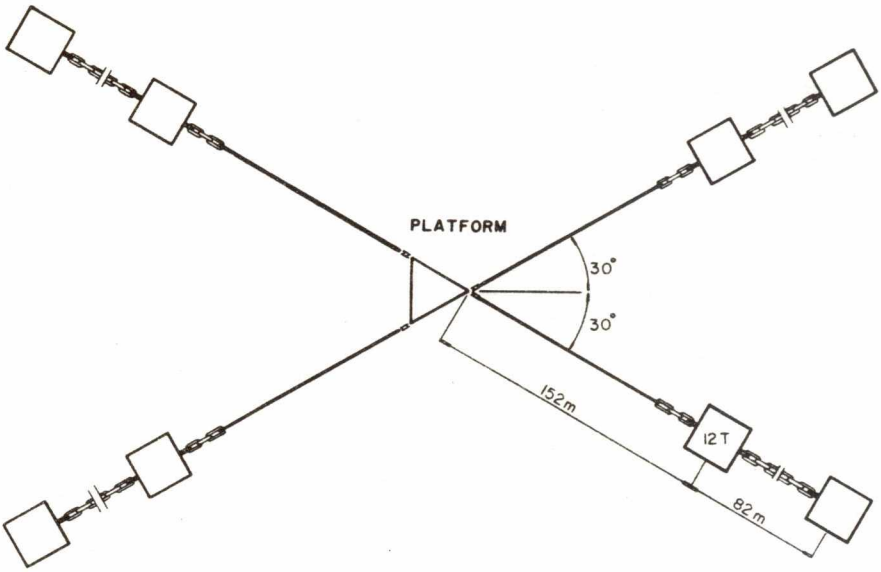

FIGURE 9: Anchor Layout

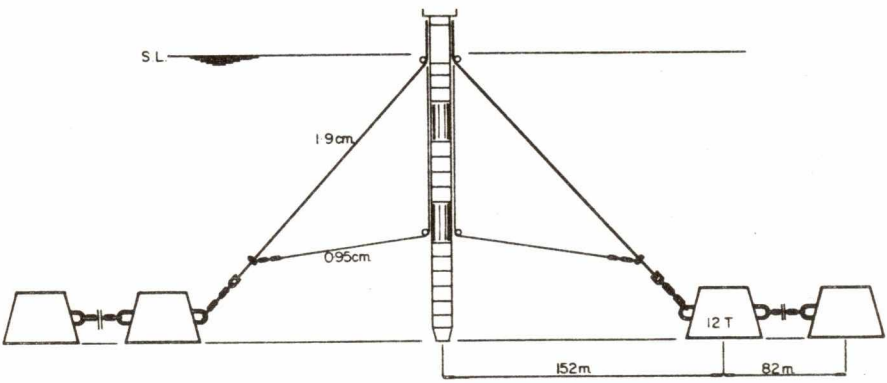

FIGURE 10: Mooring Wire System

Power for the equipment installed on the platform was provided by a submersible battery pack (Fig. 30) which was placed on the sea bed near the structure and connected by a flexible power cable. The battery pack contained nine 90-Ah automobile batteries and provided power for approximately 60 days under normal operating conditions. The battery pack could be raised and lowered from the sea bed by a small fishing boat in conditions (sea state 2) when it would have been extremely hazardous to transport batteries to the structure itself. Access to the work platform was provided by two ladders, one on each seaward leg, and it was possible to gain access to the ladders in sea state 3. To place people on the structure under these conditions required exceptional boat-handling and a maneuverable boat. A fishing boat 13.4 metres in length was very suitable for this purpose.

4. DESIGN

A principal requirement of any scientific instrument is that its presence does not disturb the phenomena being observed, a restriction which also applies to any device or structure used to hold the instrument. The holding device or structure is also subject to the limitations imposed by the instrument design. The maximum accelerations to which the AOL Mark VI wind thrust anemometer can be subjected without significantly affecting the results are horizontal 1 m/s^2, vertical 0.1 m/s^2. Therefore, the requirements of the AOL Stable Platform were that its presence did not disturb the wind and that its motion did not result in accelerations in excess of those stated above.

The most severe forces experienced by offshore structures are those resulting from the action of large waves. Ocean waves vary in height from a few centimetres to heights exceeding 30 metres but, fortunately, waves in excess of 30 metres are infrequent in most locations (in excess of a 100-year recurrence interval). In the case of an offshore instrument platform where no risk of life is involved, it is undesirable from both a practical and economic standpoint to design for the extreme case. Consequently, the choice of design wave is generally based on recorded visual observations made in the area of interest over a number of years. Data from wave recording instruments now supplements and will eventually replace visual observations. The design wave for the Mark III structure was based on data provided by Hogben and Lumb (1967), reports from local fishermen and experience with the Mark I and Mark II. The magnitude of the forces acting on the structure depend on the characteristics of the design wave and the configuration of the structure, and to minimize these forces it was necessary to keep the structure as small and streamlined as possible. This was particularly important near the water level where the wave-induced forces are most severe. The structure was designed so that wave action would have the minimum possible effect and was particularly suitable as it achieved high strength using small structural members. The method of representing the area that it presented to wave action is included in the design calculations, section 10. The magnitude of the wave force was calculated using a semi-empirical relationship proposed by Morison *et al.* (1950), which assumes that the total wave force is comprised of two parts, a drag force component dependent on friction effects and an inertial force component dependent on the inertia of the displaced fluid. This

solution can be expressed algebraically as:

$$f = 1/2\ \rho\ Cd\ D\ u^2 + \rho\ Cm\ \frac{\pi}{4} D\ \frac{du}{dt} \qquad (1)$$

drag force inertial force

f = force/ unit length (kgf/m)

ρ = mass density (kgm/m^3)

Cd = drag coefficient

u = horizontal particle velocity (m/s)

$\frac{du}{dt}$ = horizontal particle acceleration (m/s^2)

D = diameter of cylinder (m)

Cm = inertial coefficient

For member diameters less than 1.3 metres it can be shown that the drag forces are much greater than the inertial forces; and as the inertial forces occur 90 degrees out of phase, it is permissible to neglect them (Peterson, *et al.*, 1969). As the structure was constructed from pipe 0.2 metres in diameter or less over 75% of its length, the exception being the tank sections, the inertial forces were neglected. The frictional effect is directly proportional to the value of the drag coefficient Cd, a non-dimensional parameter, dependent on surface roughness, Reynolds number and the shape of the member. Its value has been determined empirically for most shapes under steady flow conditions but only limited information is available regarding suitable values for calculating wave forces. The design drag coefficient (Cd = 0.6) chosen for the Mark III was based on information provided by Myers, *et al.*, (1969). To determine the drag component of the Morison equation also requires a knowledge of the horizontal velocity of the fluid particles acting over the length of the structure. The relationship between the horizontal particle velocity u and the water depth to the second order is given by:

$$u = \frac{\pi H}{T} e^{kz} \cos\theta \qquad (2)$$

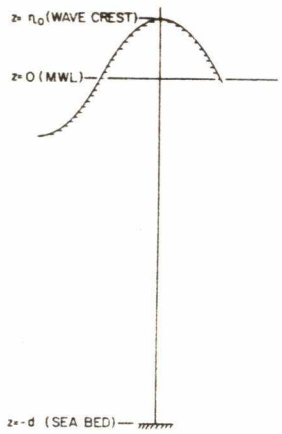

u = horizontal velocity (m/s)

H = wave height (m)

k = wave number = $\frac{2\pi}{L}$

L = wave length (m)

θ = phase position (0 at crest)

z = position relative to mean sea level

η_0 = crest height above mean sea level

$$\frac{\eta_0}{H} = \frac{1}{2} + \frac{1}{4}\left(\frac{\pi H}{L}\right)^2$$

The design calculations, section 10, show that for the design wave (height 11 metres, period 12 seconds), the overall safety factor was x2. Normal marine structures aim for a safety factor of x5 but the practical difficulties and expense involved in effecting any significant improvement given the existence of the basic structure and the availability of anchors of the type required influenced the decision to accept a low safety factor. As the safety factor was low and the loading difficult to predict from theory, the actual loading was measured using strain-gauged measuring devices in the mooring wires. The intention was to compare the actual loading with that theoretically predicted and in the event of a serious underestimate to remove the structure. Unfortunately, insufficient data was recorded under normal conditions before the arrival of the storm that caused failure.

Ocean waves and swell can contain significant amounts of energy over the frequency range 0.04 Hz (period 25 seconds) to 0.25 Hz (period 4 seconds). To minimize the danger of destructive resonance, it is desirable to ensure that the natural frequency of any offshore structure falls outside this range. The design calculations show the natural frequency in pitch of the Mark III installation to be within this critical range. This was not realized at the time of installation and discussion of the possible consequences of this oversight are included in the conclusions.

Other forces encountered in the ocean environment include those resulting from currents, winds and ice loading. The expected magnitude of these forces dependsboth on the location and the time of year. In the Mark III location these forces are insignificant in comparison to the wave force when considered on an individual basis. The possible consequences of all the forces, including wave force, acting simultaneously are discussed in the conclusions.

5. INSTALLATION

The description of the installation is divided into four parts, the placing of the concrete anchors, the preparation of the structure, the preparation of the site, and the attachment of the structure to the anchors.

5.1 Anchor Placement (see Figures 11 and 12)

The concrete anchors were placed using a floating crane, a 1000 hp tug and the vessel *Sigma-T*. The floating crane was a flat-bottomed barge 30 metres in length and 18 metres wide, fitted with a rotating boom and lifting equipment capable of lifting 100 tons. There was ample deck space for the eight 12-ton concrete anchors, the 300 metres of chain cable and the four conical mooring buoys used in the anchor layout. Ballast tanks on the barge were flooded to counteract the effect of the weight of the concrete anchors on the trim of the barge. The barge had no independent means of steerage or propulsion and was completely dependent on the tug for mobility and positioning. The tug had a maximum line pull of 8.5 tons, and the vessel *Sigma-T* was a 16.5 metre longliner fitted with Decca navigator, radar and a winch capable of lifting one ton.

The procedure for laying each of the four legs of the anchor layout was as follows. The position of the front (nearest the centre of the layout) concrete anchor was determined with the Decca navigator and marked by deploying a plastic marker buoy attached to a railroad wheel with 1.25 cm diameter polypropylene rope. To achieve accurate positioning of the front anchor, the barge was anchored 100 metres upwind of the marker buoy and allowed to drift back. The anchor was lowered on the chain cable that ultimately linked the two anchors in each leg together, and as there was no chain cable windlass on the barge, it was necessary to lower it on the boom crane hook. This was an extremely slow operation as it could only be lowered 20 metres at a time: the distance between the boom and the deck of the barge. The 1.9 cm diameter wire used to moor the structure was attached to the anchor when it was on the deck of the barge and was paid out as the anchor was lowered. The end of each mooring wire was buoyed off with a conical mooring buoy 2 metres high with a maximum buoyancy of 2 tons. With the anchor on the sea bed, the barge paid out on the chain cable while winching back to its own anchor. When the barge's anchor had been retrieved, the chain cable leading to the front anchor was winched in and attached to a second concrete anchor. The tug then towed the barge in the appropriate direction until the chain cable became taut and pulled the second anchor from the deck of the barge. It was intended to tighten the chain cable connecting the anchors by joining the tug's towline to the buoyed off mooring wire and towing the front anchor but this proved to be impractical as at the first attempt it stretched the mooring wire and made it extremely difficult to handle. Consequently, on three of the four legs of the anchor layout the connecting chains were never tightened, and the possible consequences of this are discussed in the conclusions.

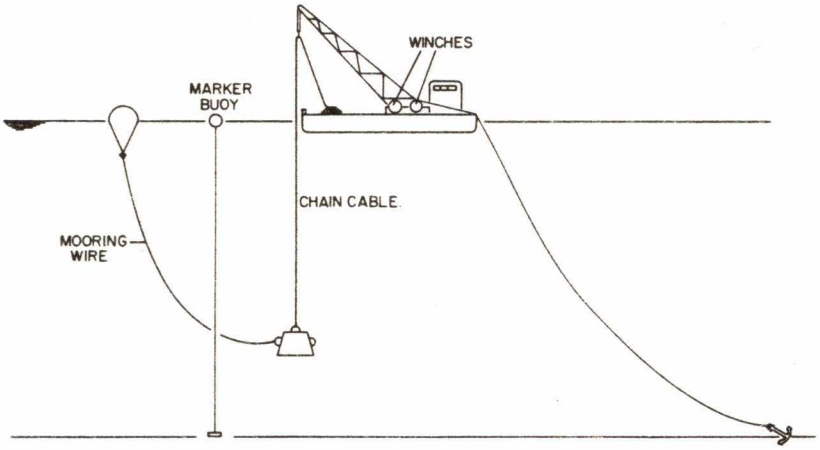

FIGURE 11: Placing Front Clump Anchor

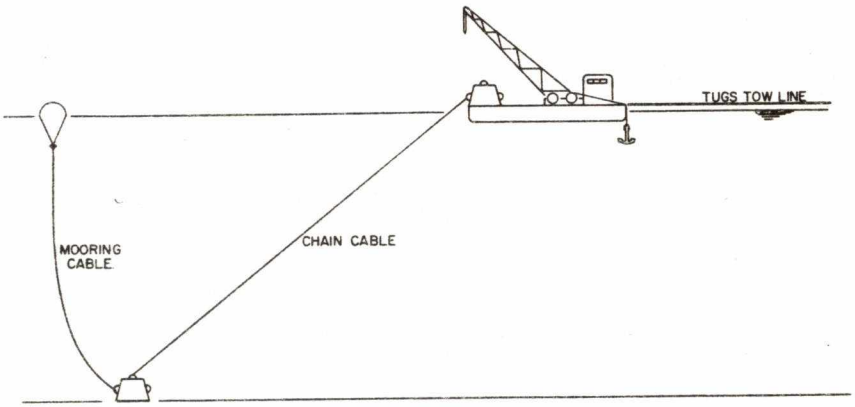

FIGURE 12: Placing Rear Clump Anchor

5.2 Preparation of Structure

Before the Mark III structure was placed in the water four 185-metre lengths of 0.95 cm diameter galvanized wire were attached as shown in Figure 7 and 13. One end of each wire was started on each of the four 5-ton hand winches installed on the work platform and the other ends were passed over the appropriate pulleys on the platform, through the swivel snatch blocks 43 metres below the platform and back up to the temporary platform 1.5 metres below. The remaining 91.5 metres of each wire were coiled and tied to the temporary platform and eyes made in the four free ends to simplify the attachment of additional 1.25 cm wires during the mooring operation. The wires running along the structure were tied off with marlin at 4-metre intervals to prevent tangling.

The structure was placed in the water using two 45-ton cranes each fitted with a 20-metre boom as shown in Figure 14 and it was then towed to a temporary mooring in the Bedford Basin to provide easy access for the tug. The lower tanks were flooded until the base section was 15 metres below the surface (Fig. 15) as experience had shown that it towed better at an angle than in the horizontal attitude. It took five hours to tow it from its mooring in the Bedford Basin to the chosen location at the maximum towing speed of 4-5 knots. The speed was governed by the performance of the structure under tow and not the capability of the tug but the wide reserve of power provided by the 1000 hp was desirable to allow for unforeseen weather conditions.

5.3 Preparation of Site

Before the structure arrived at the site, the following preparations were made to each of the four mooring wires. Each mooring buoy was lifted from the water using the boom of the *Sigma-T*. The mooring wire was unshackled from the lower eye of the buoy, passed over the fairlead roller on the stern and round the capstan-head as shown in Figure 16. When the capstan-head had recovered 6 metres of the mooring wire, the end was shackled to the upper eye of the buoy and the buoy placed in the water alongside. The capstan-head was then used to bring in the remaining slack in the mooring wire; and as it came off the capstan-head, it was passed over the side so that its weight hanging from the upper eye of the buoy eventually caused it to turn upside down. With the 1.9 cm mooring wire tight over the stern the 82.5 metres of 0.95 cm diameter galvanized wire were attached to it using a device known as a 'chain stopper'. Consisting of a one-metre length of 0.95 cm chain it was wrapped around the mooring wire so that it slid down but fetched up when pulled in the reverse direction. By shackling the 0.95 cm wire to this device, it was possible to attach it to the mooring wire 55 metres below the sea surface without divers. The mooring buoy was then pulled to the stern of the *Sigma-T* and its lower eye attached with a chain stopper to the taut portion of the 1.9 cm mooring wire. (The lower eye of the buoy was uppermost at this stage because of the weight of slack mooring wire hanging from its upper eye.) The taut portion of the mooring wire was then released causing the buoy to revert to its normal attitude, and the free end of the 0.95 cm wire was attached to the upper eye. Figure 17 shows the configuration of the mooring wire before and after the slack was removed. The removal of the slack and the attachment of the 0.95 cm wires took eight hours and was carried out

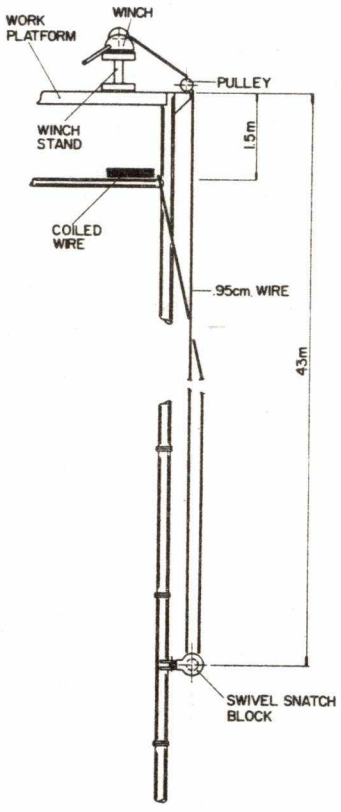

FIGURE 13: Attachment of 0.95 cm Wires to Structure

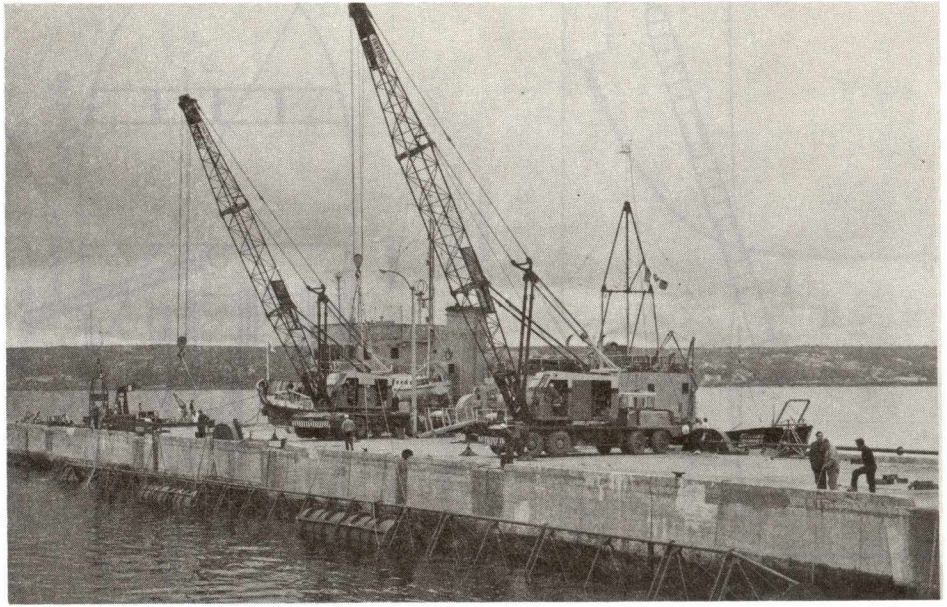

FIGURE 14: Platform Structure Being Placed in Water

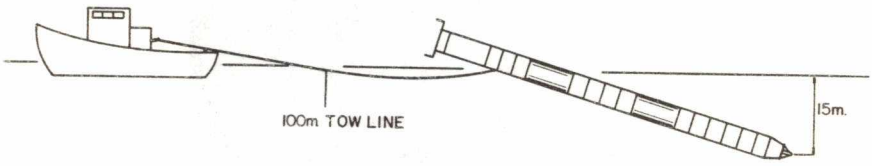

FIGURE 15: Towing Configuration

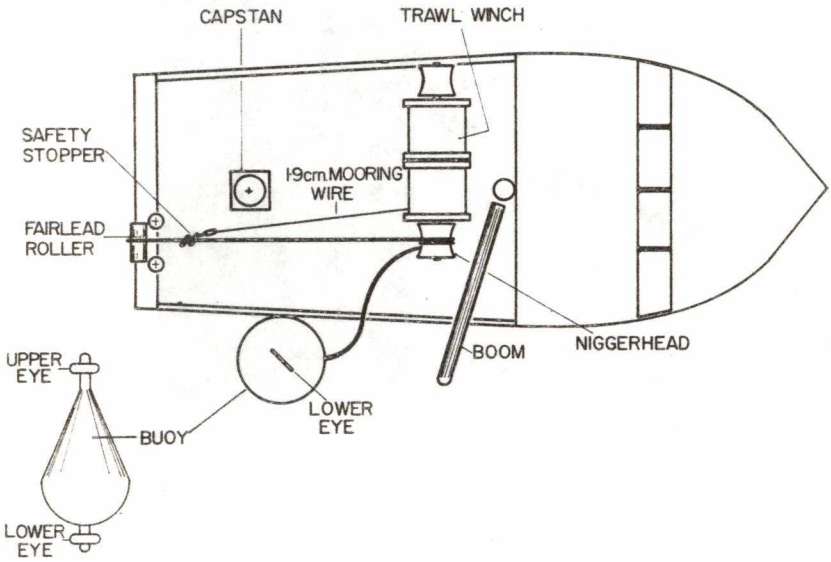

FIGURE 16: Mooring Wire Shortening

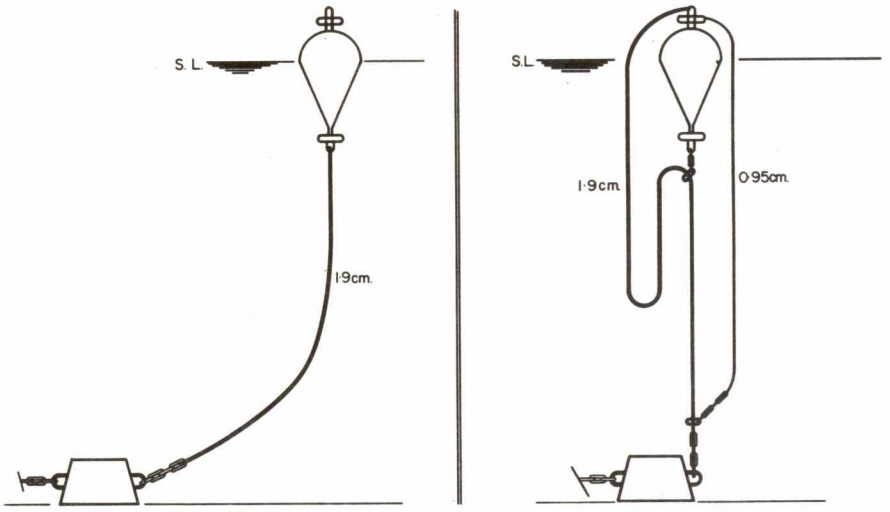

FIGURE 17: Shortened Mooring Wires

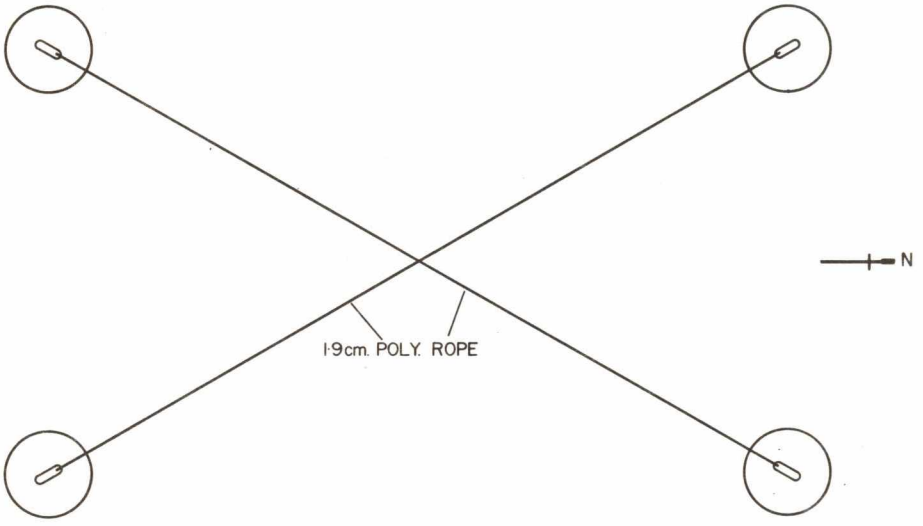

FIGURE 18: Rope Cross Layout

immediately prior to the arrival of the structure to minimize the probability of the 1.9 cm and 0.95 cm wires tangling. Finally, a 1.9 cm diameter polypropylene cross was laid between the mooring buoys as shown in Figure 18. To maximize the daylight hours available for working on the structure these preparations were made during the night.

5.4 Attachment of Mooring Lines

When the structure arrived at the location, a diver operated the lower tank valves to bring it to a 45-degree angle. The tow rope was then transferred to the *Sigma-T*, which proceeded under the rope cross until the structure reached the centre of the cross where it was correctly orientated and made fast. There was sufficient slack in the rope cross to enable the *Sigma-T* to pass underneath without difficulty. One of the 0.95 cm wires on the structure was then passed to the *Sigma-T* which proceeded to the appropriate mooring buoy, disconnected the 0.95 cm wire from the buoy, and shackled the two wires together (Fig. 19). This was repeated for all four legs of the mooring system. The hand winches were then used to bring the structure to the vertical position (Fig. 20) and the 0.95 cm wires were wire-clipped to gusset plates just below the platform at the 1.5-metre level. With the wires securely clipped to the gusset plates, the four wires were cut between the gusset plates and the winches and an eye made in each of the eight free ends. Wire stoppers were shackled into the eyes of the wires running to the winches and the other ends coiled and laid on the temporary platform at the 1.5-metre level. The *Sigma-T* then brought the mooring wires (1.9 cm diameter) from the mooring buoys to the structure and each wire was passed through the appropriate swivel snatch block at the 8.5-metre level and up to the work platform. The wire stoppers on the winch wires were then attached to the mooring wires just above the swivel snatch blocks and the winches used to tension the wires until the mooring buoys sank below the surface (Fig. 21). Divers then cut the chains holding the buoys to the mooring wires with bolt cutters and further tensioning was carried out to remove the resulting slack. The 0.95 cm wires were also tensioned at this stage, and the resulting configuration is shown in Figure 22. The lower buoyancy tanks were then completely flooded to take the structure to the bottom, and the 0.95 cm and 1.9 cm wires tensioned again (Fig. 10).

From tying to the rope cross to completion of the mooring operation took four days during which time the weather conditions were nearly perfect with conditions equal or better than sea state 2, wind velocity $\leq$ 10 knots, maximum wave height $\leq$ 1 metre.

The structure was inspected every two days for a period of two weeks, and a diver inspection confirmed that the load-bearing plate had contacted the bottom. A close check was kept on the wire tensions using a Dillon load-cell and when it became apparent that the main mooring wires were maintaining the desired mean tension of 0.75 ton, the hand winches were removed. The radio mast, transmit and receive antennas, wave staff, accelerometers, strain-gauged turnbuckles and electronics package were then installed on the structure. The performance of the structure was then monitored for a period of four weeks before the accelerometers were replaced with the thrust anemometer.

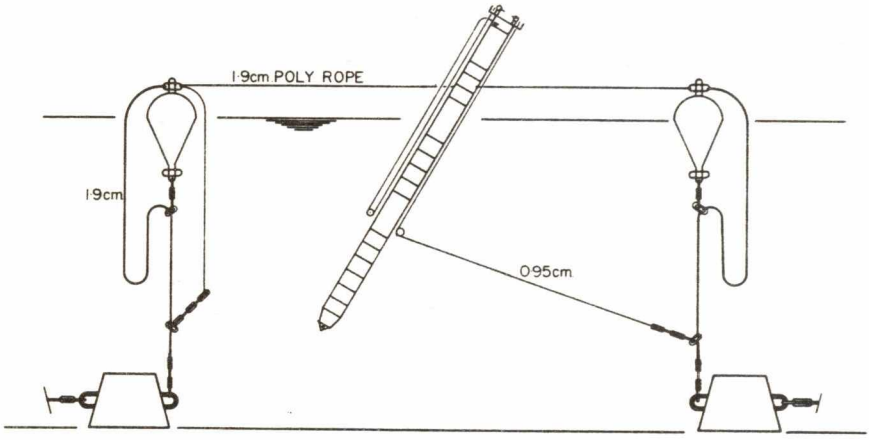

FIGURE 19: Attachment of 0.95 cm Wire

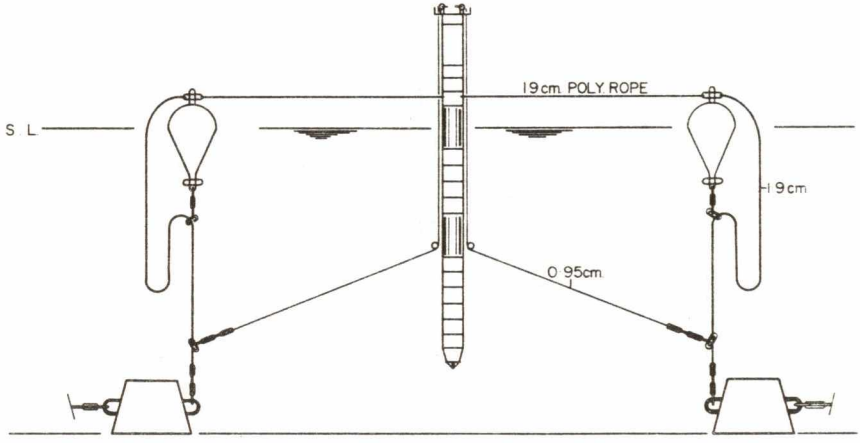

FIGURE 20: Structure in Vertical Position

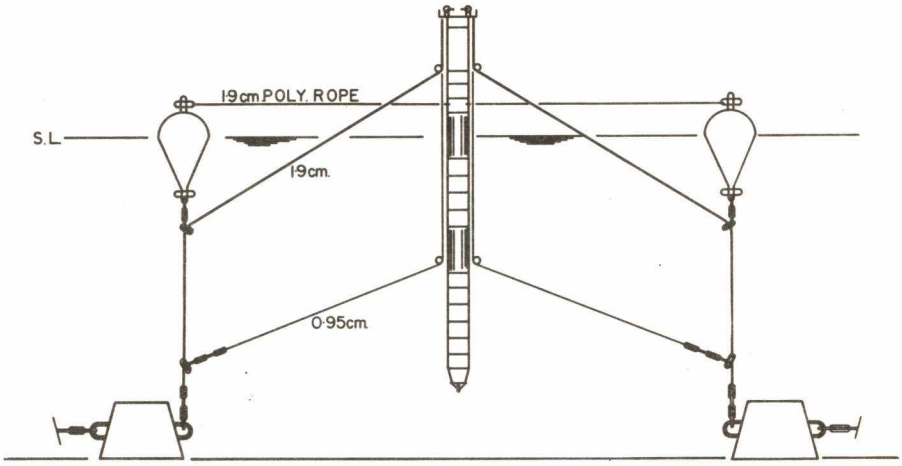

FIGURE 21: Attachment of 1.9 cm Wires

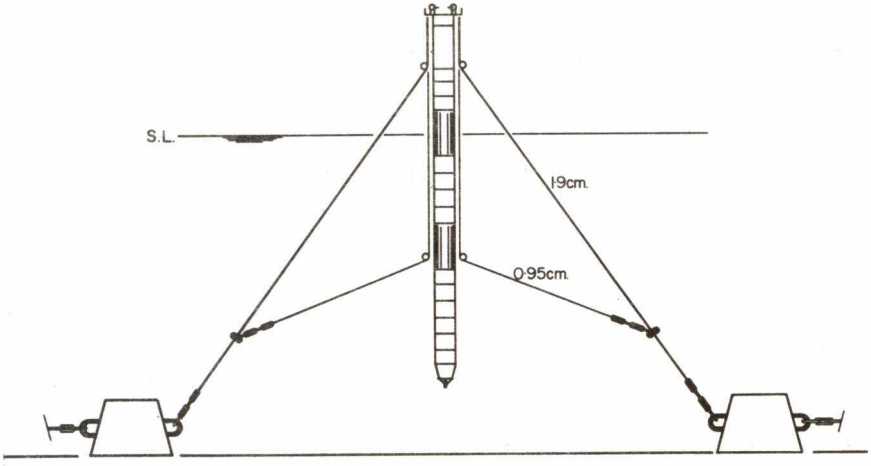

FIGURE 22: Configuration with Buoys Removed

6. DATA ACQUISITION

The following sensors (Fig. 8) were installed on the Mark III Stable Platform:

(1) The AOL Mark VI wind thrust anemometer for wind thrust measurements (Smith, 1969).

(2) An aerovane anemometer to measure wind speed and direction (Smith, 1969).

(3) A thermistor for measuring air temperature (Bendell, 1971).

(4) A wave staff to measure wave height.

(5) A three-axis accelerometer to determine the stability of the platform structure.

(6) Four turnbuckles instrumented with strain gauges to measure the tension in the mooring wires.

The frequency-modulated command and telemetry system used to control and monitor the sensors is described in detail by Dinn (1972). Brief descriptions of the command and telemetry system, the wave staff, the accelerometer package and the strain-gauged turnbuckles are included in this section as they were used to monitor the performance of the structure. Details of the underwater battery box used to power the system are also included.

6.1 Command and Telemetry System

The command and telemetry system (Fig. 23) was developed to control and monitor the sensors installed on the structure from a shore station. This was an essential requirement as it was inaccessible under the conditions of interest, storm conditions. The system had two modes of operation: operational and standby. By placing the system on standby when data was not required, the power consumption was reduced from 25 watts to 1 watt. This extended the life of the underwater battery box from 10 days under continuous operation to 60 days under normal operating conditions. The system had the capability of recording 12 channels of data simultaneously and channel numbering was in accordance with IRIG format as listed in Table 1. The allocation of channels to the sensors is given in Table 2 and a simplified block diagram (Fig. 24) illustrates the method of data collection. The output of each sensor was conditioned so that a change in sensor output resulted in a change in a d.c. voltage level. The full operational range of each sensor was represented by a voltage change of +2.5 to -2.5 volts d.c.

Each conditioned sensor output was fed, via a limiting circuit, to a voltage-controlled oscillator operating over the frequency range of one IRIG channel. The limiting circuits prevented the voltage-controlled oscillators from being overdriven, and therefore prevented the IRIG channels overlapping. The sensor outputs, in the form of varying frequencies, were then

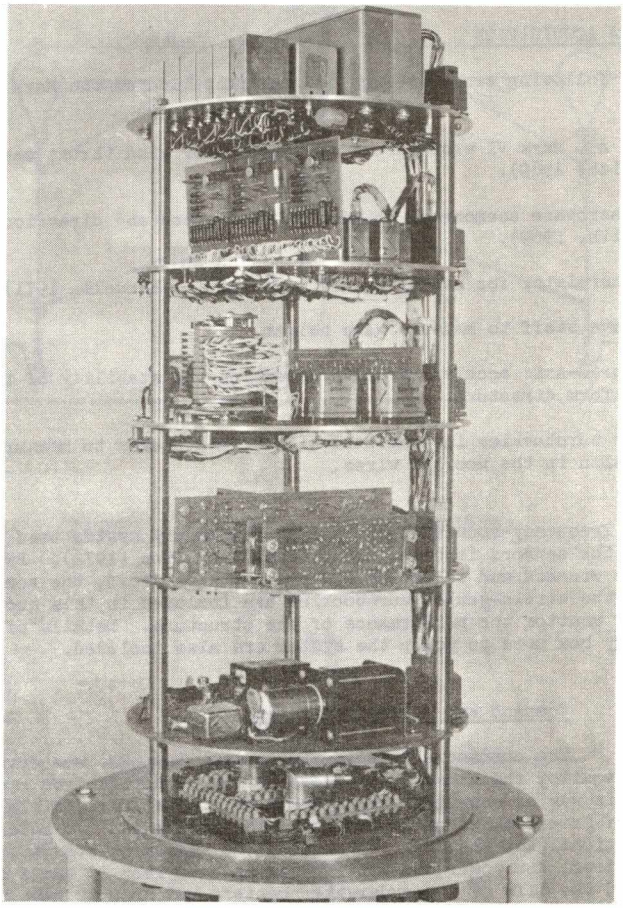

FIGURE 23: Command and Telemetry System

TABLE 1

IRIG Standard Frequencies

Channel No.	Lower Band Edge		Band Centre		Upper Band Edge		Δf
	Frequency Hz	Period μs	Frequency Hz	Period μs	Frequency Hz	Period μs	Hz
1	370	2702.7	400	2500.0	430	2325.5	60
2	518	1930.5	560	1785.7	602	1661.1	84
3	675	1481.4	730	1369.9	785	1273.9	110
4	888	1126.1	960	1041.7	1,032	968.99	144
5	1,202	831.95	1,300	769.23	1,398	715.31	196
6	1,572	636.13	1,700	588.23	1,828	547.05	256
7	2,127	470.15	2,300	434.78	2,473	404.37	346
8	2,775	360.36	3,000	333.33	3,225	310.08	450
9	3,607	277.24	3,900	256.41	4,193	238.49	586
10	4,995	200.20	5,400	185.19	5,805	172.27	810
11	6,799	147.08	7,350	136.05	7,901	126.57	1,102
12	9,712	102.97	10,500	95.238	11,288	88.590	1,576
13	13,412	74.560	14,500	68.966	15,588	64.152	2,176
14	20,350	49,140	22,000	45.455	23,650	42.283	3,300
15	27,750	36.036	30,000	33.333	32,250	31.008	4,500

TABLE 2

IRIG Channel Allocations

Channel 1	Aerovane Sine Signal
2	Aerovane Cosine Signal
3	Battery Voltage
4	Wave Height Signal
5	Tension, Turnbuckle
6	Tension, Turnbuckle
7	Tension, Turnbuckle
8	Tension, Turnbuckle
9	Air Temperature
10	Thrust Anemometer Component 1/ or Accelerometer Component 1
11	Thrust Anemometer Component 2/ or Accelerometer Component 2
12	Thrust Anemometer Component 3/ or Accelerometer Component 3

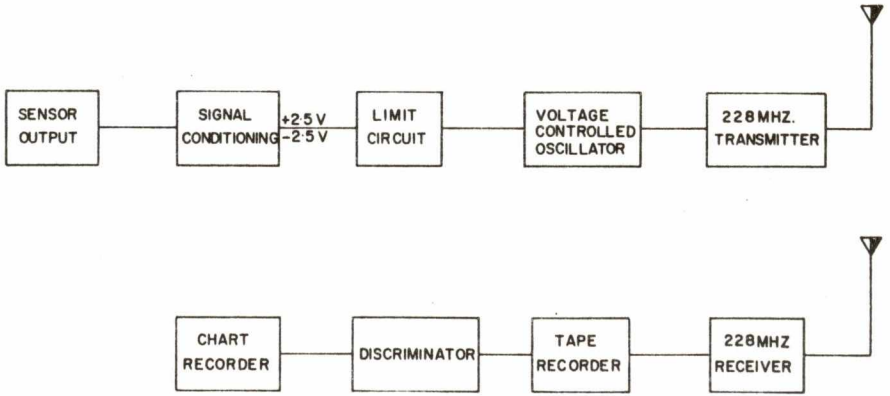

FIGURE 24: Data Collection Block Diagram

multiplexed and applied to the modulation input of a 228 MHz frequency-modulated (FM) transmitter. The frequency multiplexed signal was received at the Osborne Head recording station and recorded on analogue magnetic tape. The tape recorder was fitted with separate recording and playback heads which allowed the signal as recorded on tape to be fed into a discriminator bank. Each discriminator extracted one IRIG data channel from the multiplexed input signal, and the output of each discriminator was demodulated to produce the conditioned sensor output signals that modulated the voltage-controlled oscillators prior to transmission. The sensor outputs were displayed on a chart recorder for visual analysis and Figure 25 is an example of a chart recording. The chart recorder could only display six channels of data simultaneously, but by using a patch panel, any six of the twelve sensor outputs could be displayed.

6.2 Wave Staff

The wave staff (Fig. 26) was designed and built to AOL specifications by Nova Scotia Research Foundation.* It was constructed from a flexible nylon tube and supported vertically on the structure by a taut steel cable through its centre. The nichrome resistance wire was wound in a spiral groove cut in the outside of the nylon tube. Winding spirally increased the resistance per foot length and also permitted the wave staff to be coiled into a 1.2 metre diameter coil for easy transportation. Setting the resistance wire in a groove maintained the relative position of the wire turns and also protected the wire from abrasion. The wave staff had an active length of 12.2 metres and a total resistance of 465 ohms. Due to the conductivity of sea water the resistance wire below the sea level is shortcircuited and therefore the resistance seen alters with a change in sea level. A 12.2 metre change in sea level was converted to a 5 volt d.c. change by the wave staff electronics board.

6.3 Accelerometer Package

The accelerometer package (Fig. 27) consisted of three Kistler Model 305A servo accelerometers mounted on mutually perpendicular axes inside a canister, 13 cm diameter by 20 cm long. With the accelerometer package installed on top of the 6-metre radio mast, the acceleration data included the motion of the radio mast and the structure. The orientation of the two horizontal accelerometer axes are shown in Figure 28a. The accelerometer package electronics board was arranged to accommodate a maximum acceleration of ±0.72 g in either of the horizontal components and by use of the command telemetry system the gain of the amplifiers could be increased to provide additional full scale acceleration ranges of ±0.36 g, ±0.18 g, and 0.09 g. The vertical component had full scale acceleration ranges of ±0.144 g, ±0.072 g, ±0.036 g and ±0.018 g. To accommodate the three accelerometers three IRIG data channels were required and as the 12 data channels provided by the command and telemetry system were allocated to other sensors, the

---

* Now available from Hermes Electronics, Dartmouth, N.S.

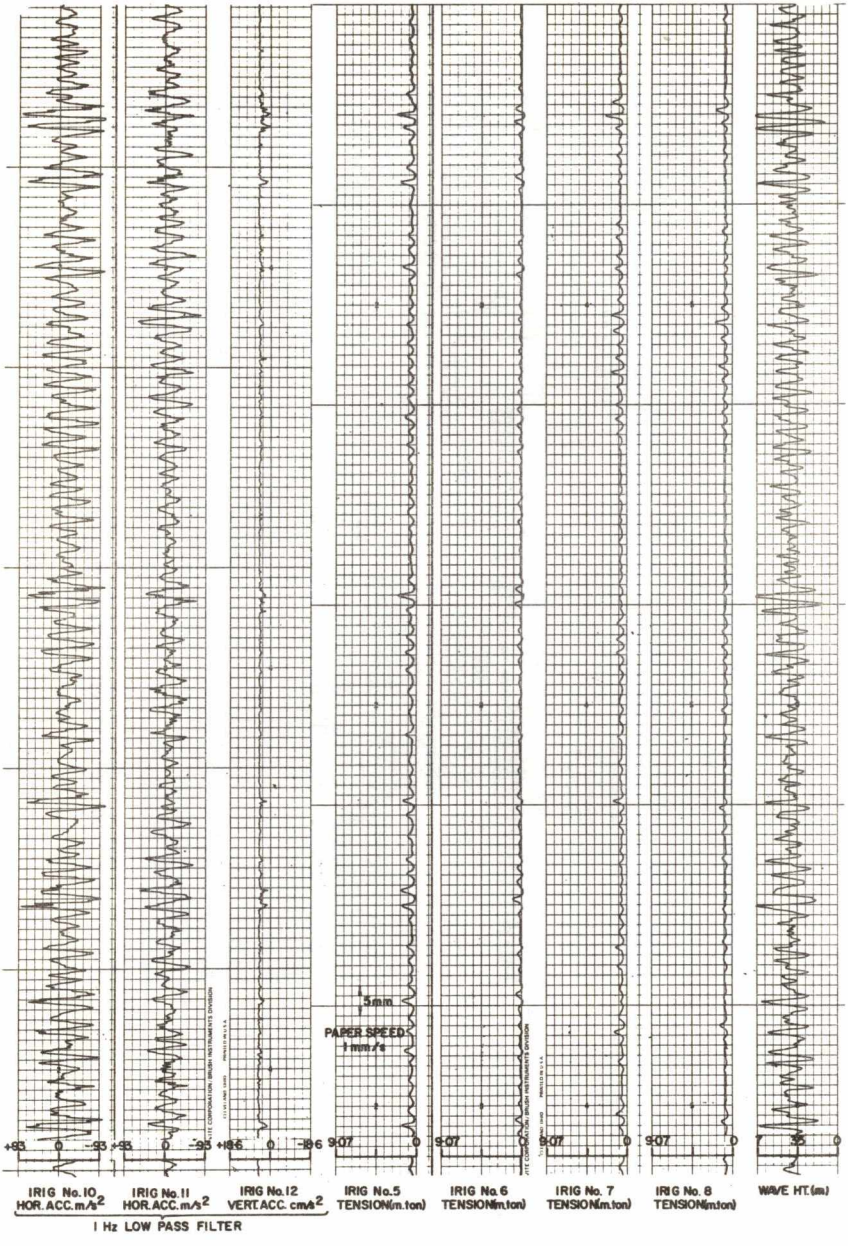

FIGURE 25: Chart Record (System Test 13)

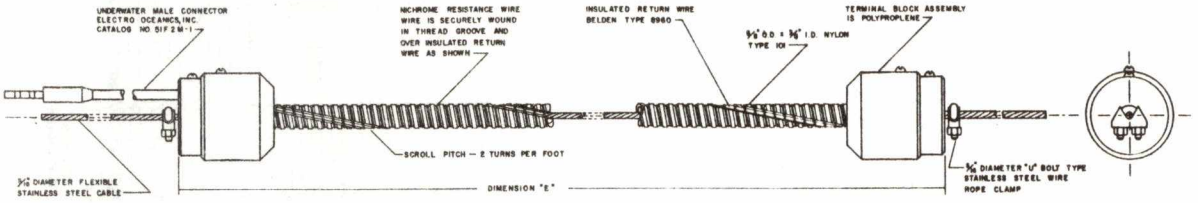

VARIABLE DIMENSION TABLE

EFFECTIVE RESISTANCE LENGTH, FT.	NICHROME WIRE DIA.	FLEXIBLE STAINLESS STEEL CABLE LENGTH, FT.	DIMENSION "E" INCHES	THREADS PER INCH	TOTAL RESISTANCE OHMS (APPROX)
20	0.0179 B&S NO.25	28	244	8	440
30	0.0179 B&S NO.25	38	364	4	440
40	0.0201 B&S NO.24	48	484	4	485

TAKEN FROM: NOVA SCOTIA RESEARCH FOUNDATION
DRAWING NO. E-1-1
PATRICK M TAIANI

FIGURE 26: Flexible Wave Staff

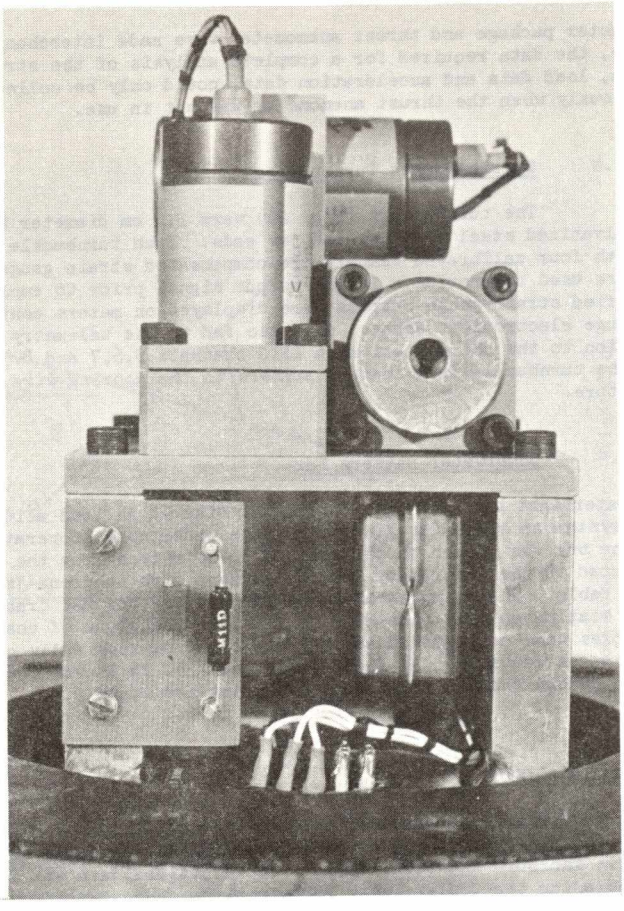

FIGURE 27: Accelerometer Package

accelerometer package and thrust anemometer were made interchangeable. Therefore, the data required for a complete analysis of the structure, i.e. wave data, load data and acceleration data, could only be collected simultaneously when the thrust anemometer was not in use.

6.4 Strain-Gauged Turnbuckles

The turnbuckles (Fig. 29) were 3.2 cm diameter by 61 cm take-up, of galvanized steel with jaw and jaw ends. Each turnbuckle was instrumented with four calibrated temperature-compensated strain gauges. Four gauges were used to provide a larger output signal prior to amplification. The amplified strain-gauge outputs were displayed on meters contained in the strain gauge electronics package, and also fed to the telemetry system for transmission to the shore station on IRIG channels 5,6,7 and 8. Figure 28b relates the turnbuckle IRIG channel numbers to the mooring wire locations on the structure.

6.5 Underwater Battery Box

A watertight box (Fig. 30) containing nine 90 Ah lead acid batteries gave the system an operation life of 60 days under normal operating conditions. The box was placed on the sea bed 20-30 metres from the structure and connected to the instrument control package with neoprene-jacketed four-conductor cable. The output voltage of the battery box was transmitted to the shore station on IRIG channel 3 to indicate the state of charge. Two battery boxes were constructed so that one could be kept fully charged for substitution as required. As each box weighed 350 kg it was inadvisable to attempt to change them in conditions exceeding sea state 2.

7. DATA ANALYSIS

Each of the 12 channels of information in analogue format was converted to digital format using an analog-to-digital converter (Smith and Brown, 1971; Thorburn and Dinn, 1971). The digitized data was Fourier transformed using the Cooley-Tukey FFT algorithm, and power spectra of all variables were obtained together with the standard deviation of each spectral estimate (Dobson and Brown, 1972). Table 3 is a summary of the data from all system tests and data runs, system tests referring to runs made while the accelerometer package was installed (November 1970) and data runs to runs made after it was replaced by the thrust anemometer (December 1970). Table 3 includes the data obtained from the instruments on the structure, and wind and wave data from the Marine Area Forecaster, Maritime Command, Halifax.

Figures 31, and 32a and 32b show the loading in the mooring wires, the measured wave height and period, and the forecast wave height and direction for all the analyzed system tests and data runs. The resultant tension of the two wires which exhibited the maximum change in tension is shown, and this value when corrected for the wire angle gives the magnitude of the wave loading corresponding to the passage of the wave crest. The value given is not the total wave loading on the structure since a portion of the loading

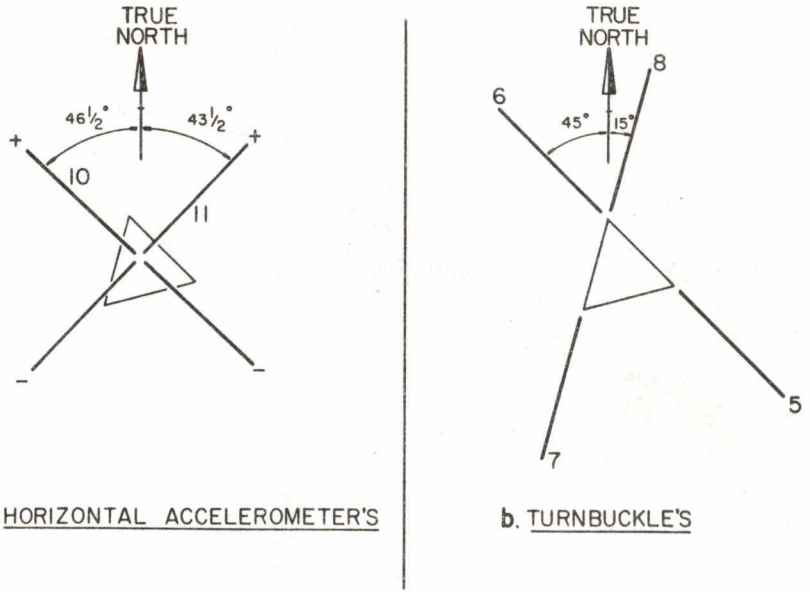

FIGURE 28: Turnbuckle and Accelerometer Orientation

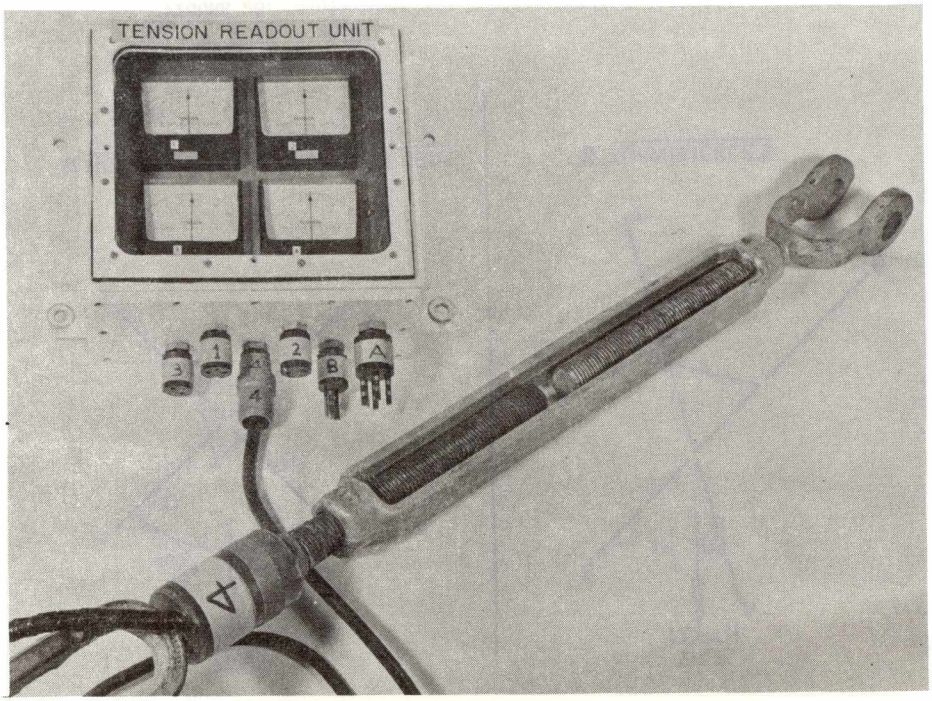

FIGURE 29: Strain-Gauged Turnbuckles

	RUN INFORMATION				WIND SPEED (m/s) & DIRECTION (true)				WAVES (m)							
					FORECAST		MEASURED.		FORECAST			MEASURED				
	RUN NO.	DATE 1970	GMT	ANALYSIS DATE	AVER. SPEED	AVER. DIRECTN	AVER. SPEED	AVER DIRECT.	SIG.	MAX. 1.8 SIG	DIRECTN (TRUE)	PERIOD	RMS	MIN.	MAX.	RANGE
SYSTEM TESTS	2	NOV. 3		6.07.71	6.7	000	15.5	354	3.3	5.9	ESE	5.20	0.50	-1.57	1.85	3.42
	3	4	19.15	19.08.71	3.5	247	7.3	234	1.5	2.7	NW	9.45	0.32	-1.00	1.38	2.38
	4															
	5	6	18.16	17.08.71	4.1	270	5.5	287	2.0	3.6	W	10.90	0.81	-2.25	2.39	4.63
	6	9	14.51	9.11.70	1.75	000	5.7	060	0.5	0.9	NW		0.24	-0,74	1.15	1.89
	7	12	14.23	22.06.71	3.1	090	6.9	066	1.5	2.7	E		0.58	-1.73	2.24	3.98
	8	13	16.43	22.06.71	3.5	000	3.1	333	1.0	1.8	NE		0.36	-0.97	1.14	2.11
	9	16	19.56	15.07.71	3.8	293	0.4	023	1.5	2.7	S	6.00	0.54	-1.40	1.45	2.91
	10	18	17.44	16.12.71	2.0	337	3.0	335	0.5	0.9	NW	9.43	0.20	-0.62	0.62	1.24
	11															
	12	20	18.28	24.02.71	2.2	000	2.3	105	1.0	1.8	NE	6.00	0.41	-1.28	1.32	2.60
	13	21	15.08	26.02.71	7.9	135	14.3	142	2.8	5.0	SE	6.90	0.97	-2.84	2.88	5.72
	14	23	15.19	12.08.71	7.5	157	24.6	165	2.3	4.1	SSW					
	15	26	17.51	29.07.71	6.2	000	11.5	004	4.3	2.3	N					
	16															
DATA RUNS	1	NOV 10	14.35	17.11.70	3.5	135	5.6	039	0.5	0.9	E	4.90	0.31	-0.93	1.05	1.97
	2	DEC 1	17.48	13.12.71	3.6	337	5.8	346	0.5	0.9	NNE	8.60	0.21	-0.67	0.87	1.54
	3															
	4	3	19.23	23.12.70	5.1	270	9.9	259	1.5	2.7	W	6.25	0.39	-1.30	1.29	2.59
	5	4	19.04	12.06.71	5.2	090	12.7	166	1.3	2.2	SW	6.25	0.55	-1.92	2.31	4.24
	6	4	23.20	15.12.71	5.2	090	7.7	198	1.5	2.7	SW	6.90	0.63	-2.22	2.04	4.25
	7	5	16.50		8.0	315	13.1	320	2.0	3.6	W					
	8	10	15.10		8.2	090	10.5	097	2.5	4.5	SE					
	9	10	16.22		8.2	090	9.7	092	3.0	5.4	ESE					
	10	10	18.11		8.2	090	12.5	071	3.0	5.4	ESE					
	11	10	19.12		8.2	090	12.4	056	3.0	5.4	ESE					
	12	10	20.02		8.2	090	13.9	059	3.0	5.4	ESE					
	13	11	15.36		5.7	337	9.6	324	2.0	3.6	NW					
	14	18	21.02	16.04.71	7.4	315	9.0	282	2.9	5.2	SSW	9.45	0.94	-2.29	2.90	5.19
	15	20	19.35	17.02.71	6.2	315	9.8	280	1.3	2.3	NW		0.42	-1.42	1.60	3.02
	16	20	20.34	1.02.72	6.2	315	8.7	285	1.0	1.8	NW	8.60	0.42	-1.42	1.54	2.96
	17	21	16.31		8.9	293	13.1	298	1.5	2.7	W	6.75	0.40	-1.31	1.76	3.07

	TENSION (kg x 100)																			
	IRIG NO. 5					IRIG NO. 6					IRIG NO. 7					IRIG NO. 8				
RUN NO.	MEAN	RMS	MIN.	MAX.	RANGE	MEAN	RMS	MIN.	MAX.	RANGE	MEAN	RMS	MIN.	MAX.	RANGE	MEAN	RMS	MIN.	MAX.	RANGE
2	2.98	0.25	-129	1.18	2.46	3.69	0.23	-1.25	1.55	2.80						5.67	0.69	-1.52	3.80	5.32
3	3.24	0.14	-1.17	5.97	7.14	4.67	0.14	-1.21	4.30	5.52						4.00	0.32	-2.00	3.75	5.81
4																				
5	3.36	0.79	-2.08	4.27	6.34	3.87	0.79	-2.80	9.22	12.02						4.16	2.26	-3.67	17.77	21.44
6		0.16	-0.95	4.65	5.50		0.10	-1.12	4.38	5.50							0.12	-1.10	4.68	5.78
7	4.55	1.35	-3.32	6.21	9.53	3.55	0.60	-2.14	3.42	5.56						5.74	0.55	-1.91	4.42	6.32
8	4.42	0.77	-2.19	2.10	4.28	4.03	0.37	-1.16	1.38	2.54						5.93	0.29	-0.93	1.33	2.26
9	4.54	0.79	-2.38	2.78	5.16	3.82	0.34	-1.43	2.87	4.31						5.94	1.19	-2.87	7.63	10.50
10	3.73	0.23	-0.79	1.29	2.08	4.68	1.10	-3.40	2.22	5.62	7.08	0.7	-1.67	3.03	4.70	6.47	0.41	-1.72	2.04	3.75
11																				
12	7.70	1.51	-3.26	7.23	10.50	5.62	0.83	-3.01	4.57	7.58	7.59	0.68	-1.69	3.19	4.88	7.08	0.46	-1.22	2.33	3.55
13	6.15	2.55	-4.46	15.94	20.39	3.67	1.43	-3.40	14.60	18.00	8.16	1.92	-3.80	18.76	12.62	8.18	1.47	-8.99	11.44	20.43
14	6.41	0.81	-2.22	3.84	6.06	3.75	0.35	-1.53	9.99	11.52	9.40	1.54	-3.10	9.41	12.51	6.72	0.53	-1.61	6.48	8.09
15	4.27	0.72	-2.56	3.24	5.80	2.44	0.39	-1.54	2.74	4.28	6.13	0.40	-1.08	1.54	2.63	6.53	0.58	-1.72	3.65	5.37
16																				
1	4.56	0.31	-1.36	1.31	2.67	3.86	0.14	-0.83	0.61	1.44						5.70	0.14	-0.90	0.76	1.66
2	7.19	0.63	-2.30	2.99	5.29	6.25	0.41	-1.74	2.33	4.07	7.54	0.32	-0.90	2.68	3.58	7.66	0.51	-1.33	4.63	5.97
3																				
4	7.01	0.38	-1.69	1.79	3.48	7.28	0.39	-1.55	2.06	3.61	8.45	0.86	-2.35	6.79	9.14	7.67	0.62	-2.46	5.64	8.10
5	8.18	1.09	-3.74	8.29	12.03	6.88	0.91	-4.42	5.20	9.62	11.22	0.86	-2.61	5.16	7.77	7.65	0.43	-1.63	3.34	4.97
6	7.62	1.43	-3.85	7.03	10.89	6.58	1.43	-4.54	6.54	11.08	9.73	1.83	-5.06	17.00	22.06	7.92	1.29	-3.75	12.40	16.15
7	4.55	0.80	-3.54	6.39	9.93	3.55	0.72	-3.25	4.64	7.89	7.95	1.65	-4.98	14.12	19.10	8.08	3.76	-5.56	33.76	39.32
8	5.73	3.01	-4.12	23.87	27.99	4.08	1.75	-3.49	14.58	18.07	10.56	2.53	-5.81	25.48	31.29	9.72	3.42	-6.33	28.90	35.23
9	5.17	3.39	-4.40	26.79	31.19	3.23	1.94	-3.66	12.63	16.29	9.69	1.96	-4.46	12.6	17.06	9.23	3.51	-5.96	20.79	26.75
10	4.76	4.16	-5.12	34.34	39.46	1.91	1.96	-3.56	17.88	21.43	7.87	1.54	-3.84	10.25	14.09	9.26	4.38	-7.31	26.66	33.97
11	4.68	3.41	-5.17	25.22	30.49	1.67	1.25	-3.05	10.05	13.10	7.40	1.20	-2.89	7.13	10.62	9.67	3.84	-7.50	19.75	27.25
12	5.81	3.28	-5.60	21.36	26.96	2.36	1.07	-2.82	7.65	10.47	7.90	1.06	-2.92	7.75	10.67	10.72	3.93	-7.30	21.92	29.22
13	3.00	0.71	-2.49	3.16	5.65	2.64	0.49	-2.20	2.72	4.92	7.06	0.87	-2.46	5.55	8.01					
14	6.34	0.60	-2.71	2.75	5.76	12.02	1.23	-3.27	5.20	8.47	7.13	4.82	-6.12	28.26	34.38	6.12	3.38	-5.34	2.36	28.94
15											6.17	1.14	-4.58	8.16	13.19	3.71	0.42	-2.00	4.91	6.91
16	4.48	0.30	-0.84	1.06	1.90	2.51	0.07	-0.36	1.15	1.51	6.00	1.29	-4.48	6.82	11.30	3.76	0.48	-1.40	3.43	4.83
17	2.66	0.28	-0.50	1.85	2.35	1.71	0.14	-0.44	1.31	1.75	5.34	0.63	-3.26	4.50	7.76	3.91	0.30	-0.9	2.71	3.61

ACCELEROMETERS															
IRIG NO. 10 (m/s²)					IRIG NO. 11 (m/s²)					IRIG NO. 12 (cm/s²)					
MEAN	RMS	MIN.	MAX	FREQ.	MEAN	RMS	MIN.	MAX.	FREQ.	MEAN	RMS	MIN.	MAX.	FREQ.	RUN NO.
															1
-0.18	0.18	-0.82	0.82	0.145 6.17	-0.17	0.20	-0.84	0.89	0.08 4.62	8.44	0.47	-6.93	1.92	0.145 8.22	2
-0.13	0.12	-0.61	0.43	0.106 6.17	-0.06	0.15	-0.67	0.76	0.106 4.62	8.18	0.25	-3.78	3.43	0.106 8.22	3
															4
0.04	0.07	-0.36	0.33	0.106 6.17	0.02	0.02	-0.44	0.40	0.08 4.62	2.34	0.29	-3.14	1.75	0.08 8.22	5
0.21	0.09	-0.70	0.38	0.106 6.17	0.10	0.08	-0.41	0.40	0.106 4.62	7.78	0.14	-1.23	1.78	0.106 ----	6
															7
															8
															9
-0.39	0.16	-0.61	1.36	0.106 6.17	-0.13	0.16	-0.88	1.11	0.106 4.62	7.62	0.85	-13.92	4.68	0.145 8.22	10
															11
-0.36	0.16	-0.66	0.78	0.106 6.17	-0.12	0.16	-0.91	1.01	0.106 4.62	7.11	0.37	4.42	4.76	0.106 8.22	12
-0.26	0.32	-0.76	1.20	0.145 6.17	-0.05	0.29	-0.98	1.01	0.145 4.62	5.89	1.03	-10.46	5.64	0.145 8.22	13
-0.06	0.05	-0.20	0.28		-0.02	0.54	-0.25	0.30		1.39	0.12	-0.87	0.74		14
-0.33	0.14	-0.67	0.83	0.106 6.17		0.17	-0.63	0.76	0.145 4.62	10.17	0.40	-3.94	3.04	0.145 8.22	15
															16
															1
															2
															3
															4
															5
															6
															7
															8
															9
															10
															11
															12
															13
															14
															15
															16
															17

TABLE 3: Data Summary

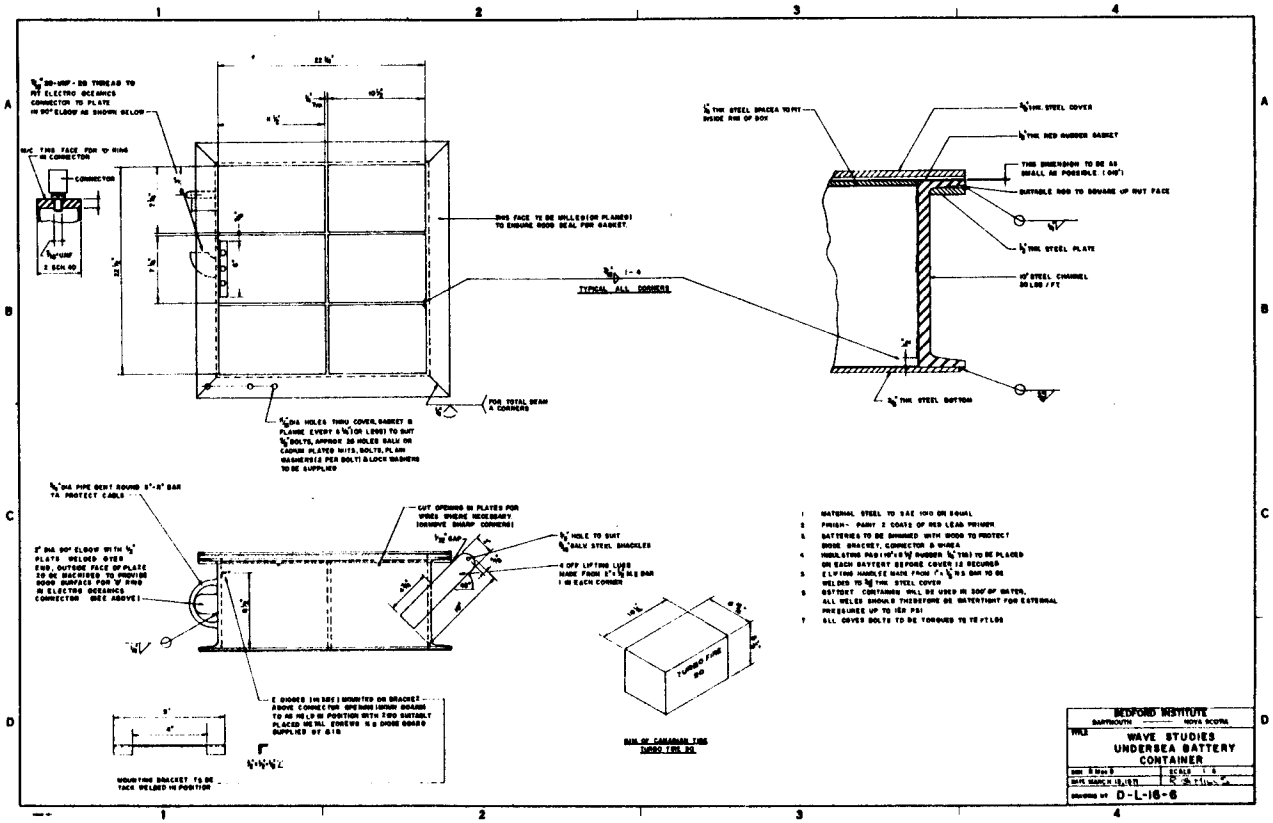

FIGURE 30: Underwater Battery Box

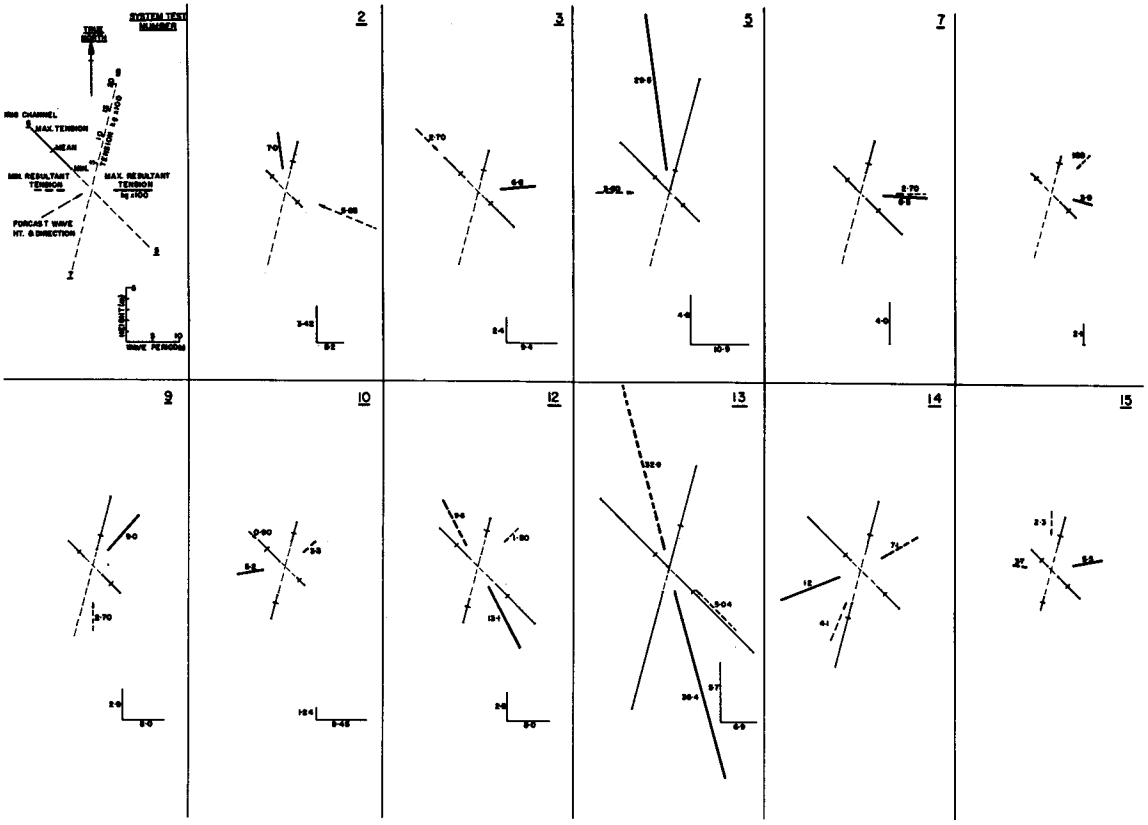

FIGURE 31: System Test Load Data

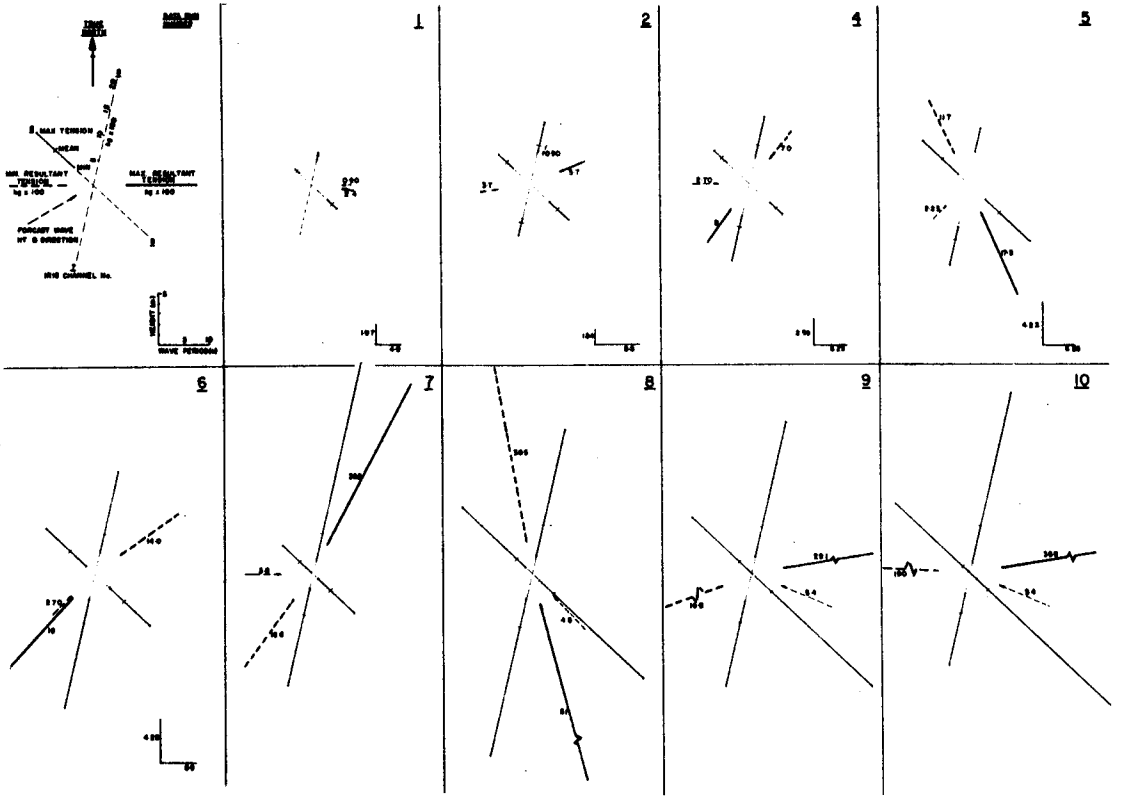

FIGURE 32a: Data Run Load Data

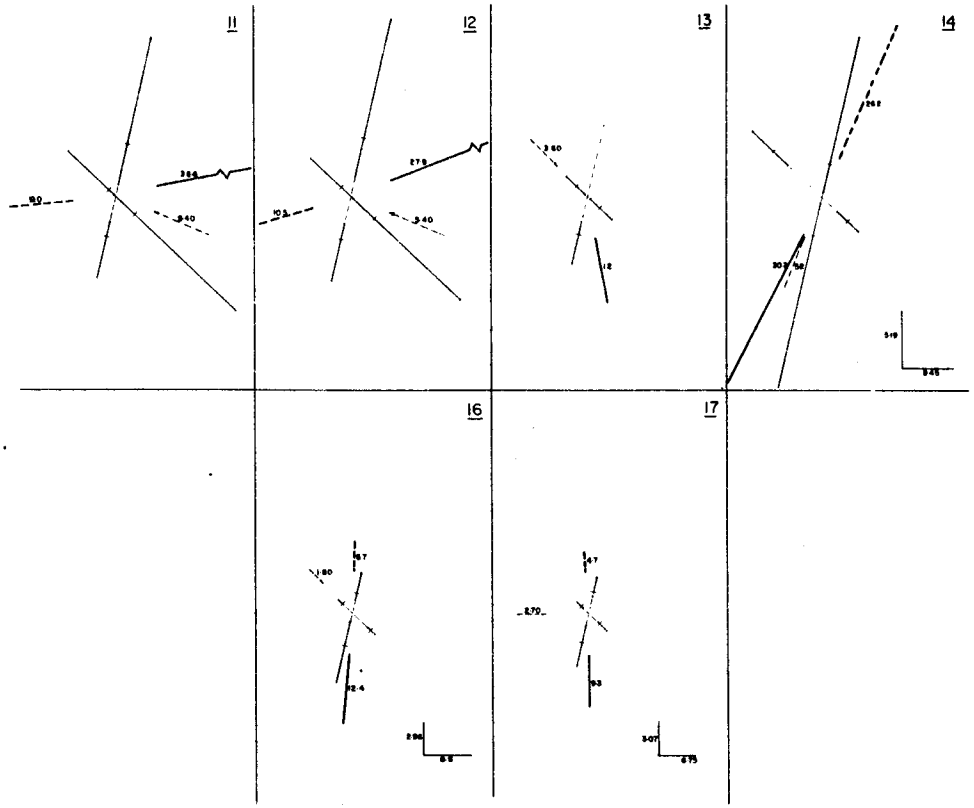

FIGURE 32b: Data Run Load Data

is taken by the reaction at the base section. Similarly the resultant tension of the two opposite mooring wires corrected for the wire angle gives the wave loading corresponding to the passage of the wave trough. The difference in direction between the two resultant tensions provides an indication of the twist in the platform's motion and the difference in magnitude to the percentage of the wave loading contained between the trough and the crest. The mean direction of the resultant tensions is the best estimate of the direction of wave motion with the waves travelling from the high resultant tension side to the low resultant tension side. Table 4 compares the estimated and forecast wave directions and the measured and forecast wave height. Figure 33 is a logarithmic plot of the maximum resultant tension against wave height for both the system tests and data runs. The slope gives the power law relationship between the two variables; that is, if $y = x^n$, the slope gives the value of n. It is assumed that the maximum and minimum tension values in each wire occur in response to the same wave, the maximum wave, and that the maximum tension change occurred in the four mooring wires simultaneously. Figure 34 shows the accelerations in the horizontal and vertical directions, the measured wave height and period, the direction of the measured waves as obtained from analysis of the tension data, and the forecast wave height and direction. The maximum and minimum resultants of the horizontal acceleration components are shown together with their mean direction. The difference in direction of the two resultants is a second indication of the amount of twist in the platform's motion, and the mean direction is the best estimate of the direction of platform motion. It is assumed that the maximum and minimum accelerations occurred in response to the same wave, the maximum wave, and that they occurred in all three components simultaneously.

To investigate the effect of the natural pitch frequency on the response of the structure to wave loading the response was approximated to that of a single degree of freedom system to a simple harmonic driving force. Figure 35 shows the theoretical response of such a system for various values of damping ratio and Figure 36 is a logarithmic plot of the most reliable data obtained on the resultant tension (wave loading)/wave height relationship before and after correction for the effect of the natural frequency in pitch. Figure 37 compares the corrected tension/wave height relationship with the theoretical value calculated using a drag coefficient Cd value of 0.6.

8. RESULTS

The Mark III Stable Platform was installed at the entrance to Halifax Harbour at the beginning of October 1970 and remained operational until a severe storm late in December caused failure, and left the structure floating at an angle of approximately 5 degrees to the vertical and attached to two mooring wires only, the northwest and southwest wires. Its position relative to the mooring wires indicated that it had moved from its original location, and an investigation by divers revealed that the base section had failed as a result of this movement. Excepting the base section, the structure was intact; but the radio mast had disappeared taking with it the thrust

SYSTEM TEST OR DATA RUN NO.	MEASURED WAVE HEIGHT M	FORECAST WAVE HEIGHT M	% ERROR = FORECAST−MEASURED/FORECAST	ESTIMATED DIRECTION DEG. TRUE	FORECAST DIRECTIDN DEG. TRUE	ERROR DEGREES
S.T. 2	3.42	5.85	+41.5	352	112	120
3	2.40	2.70	+11.1	084	315	129
5	4.60	3.60	-27.8	353	270	83
7	4.00	2.70	-48.0	D94	090	04
8	2.10	1.80	-16.7	105	045	60
9	2.90	2.70	- 7.4	042	180	138
10	1.24	D.90	-37.8	260	315	55
12	2.60	1.80	-44.5	153	045	108
13	5.72	5.04	-13.5	175	135	40
14				249	202	47
15				080	000	80
D.R. 1	1.97	0.90	-119	099	090	09
2	1.54	0.9D	-71.5	068	022	46
4	2.59	2.70	+ 4.1	216	270	54
5	4.23	2.25	-88	156	225	69
6	4.25	2.70	-57.5	223	225	02
7				028	270	118
8				165	135	30
9				D84	112	28
10				081	112	31
11				079	112	33
12				069	I12	43
13				170	315	145
14	5.19	5.20	+ 0.02	207	202	05
16	2.96	1.80	-64.5	185	315	130
17	3.07	2.70	-13.7	180	270	90

TABLE 4: Comparison Between Estimated and Forecast Wave Direction and Wave Height

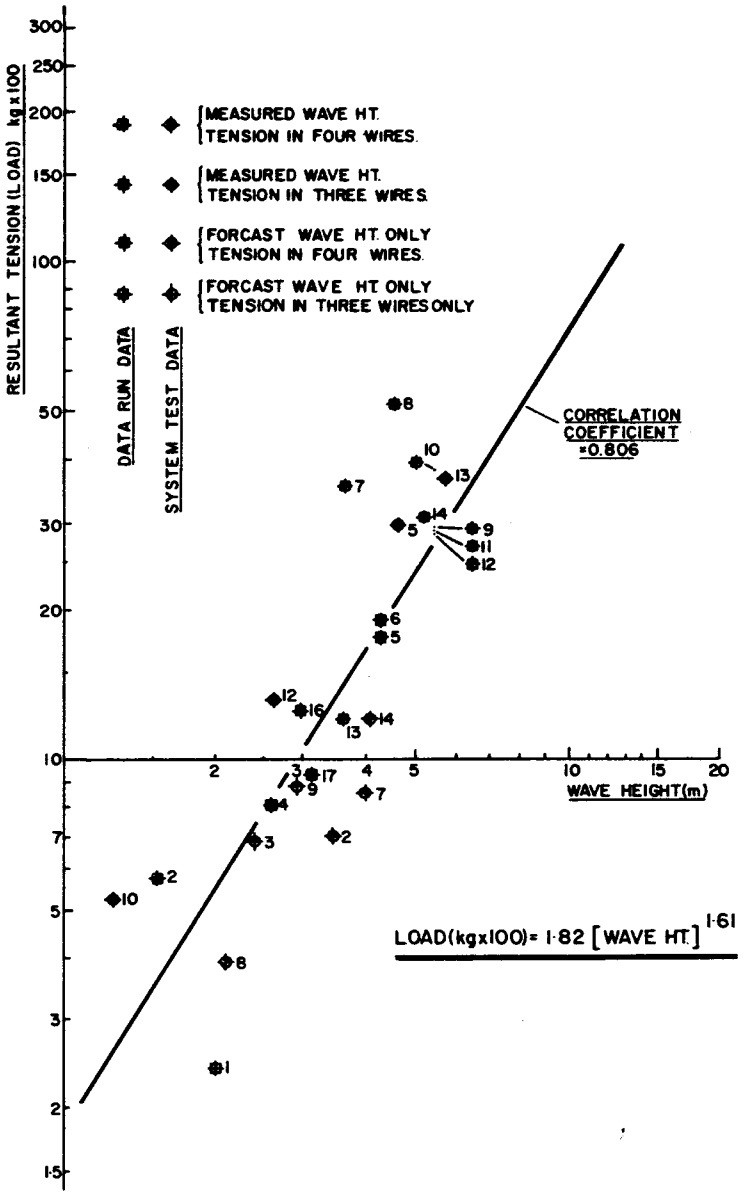

FIGURE 33: Resultant-Tension versus Wave Height-Graph for all ST and DR

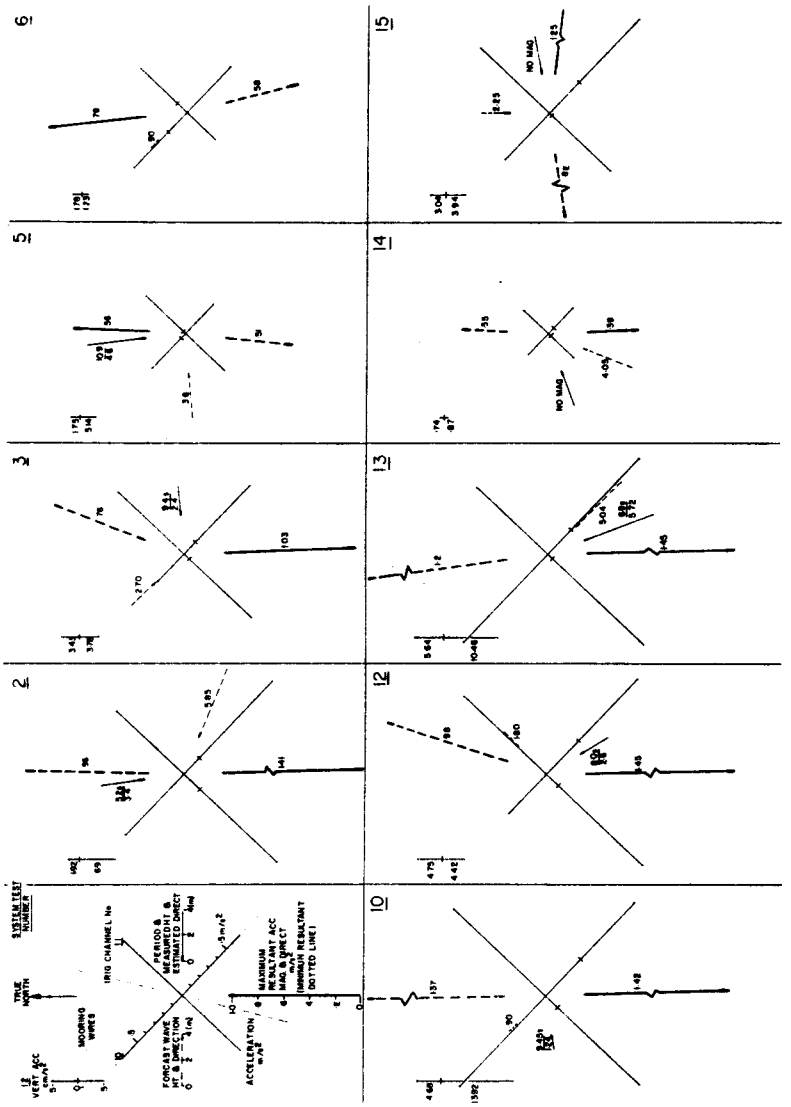

FIGURE 34: System Test Acceleration Data

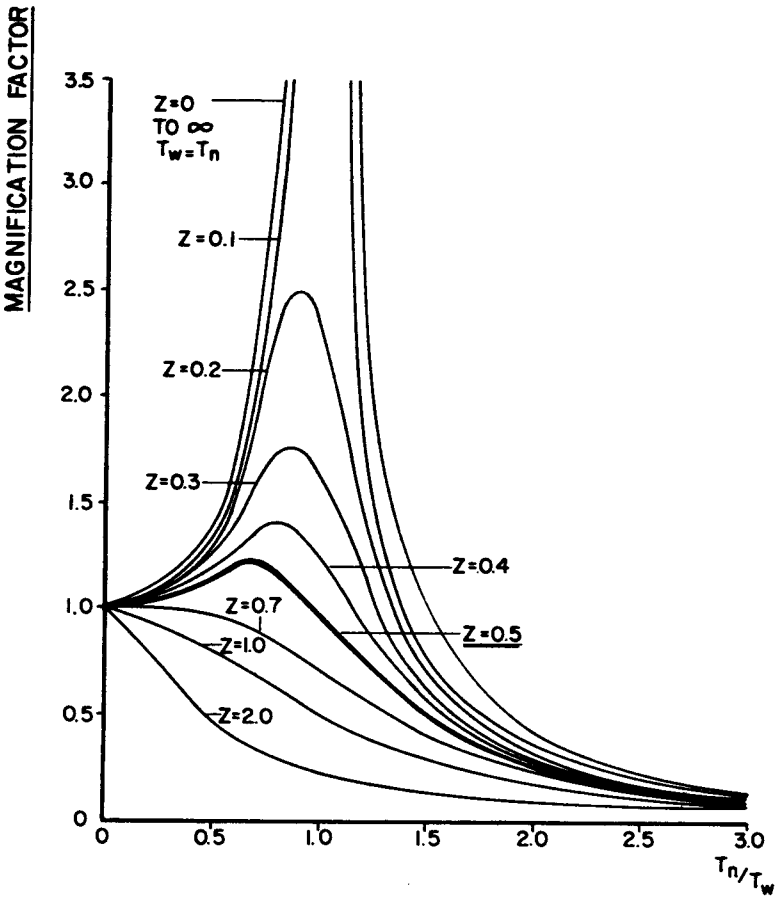

RESPONSE OF A SECOND ORDER SYSTEM WITH UNDAMPED NATURAL PERIOD T_n TO A SIMPLE HARMONIC INPUT WITH PERIOD T_w (WAVE PERIOD) FOR VARIOUS VALUES OF DAMPING RATIO Z

$$\text{MAG. FACTOR} = \frac{1}{\sqrt{\left[1-(T_n/T_w)^2\right]^2 + 4Z^2(T_n/T_w)^2}}$$

FIGURE 35: Theoretical Response to S.H. Input

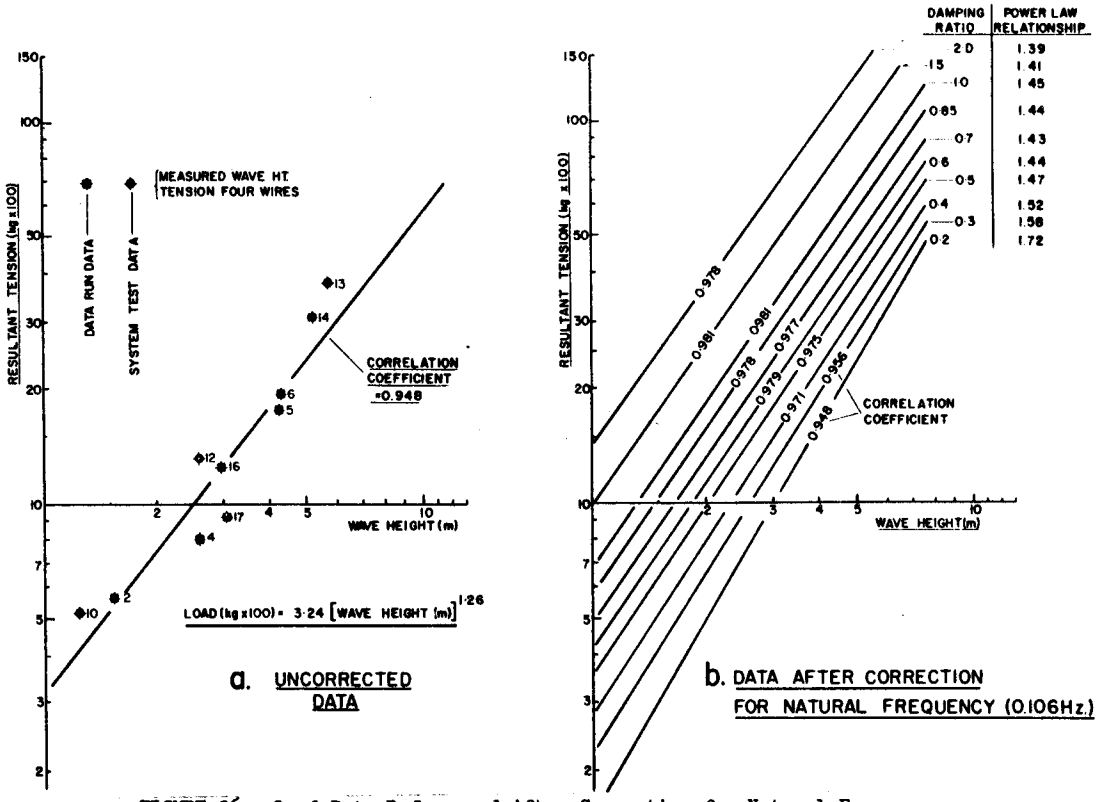

FIGURE 36: Load Data Before and After Correction for Natural Frequency

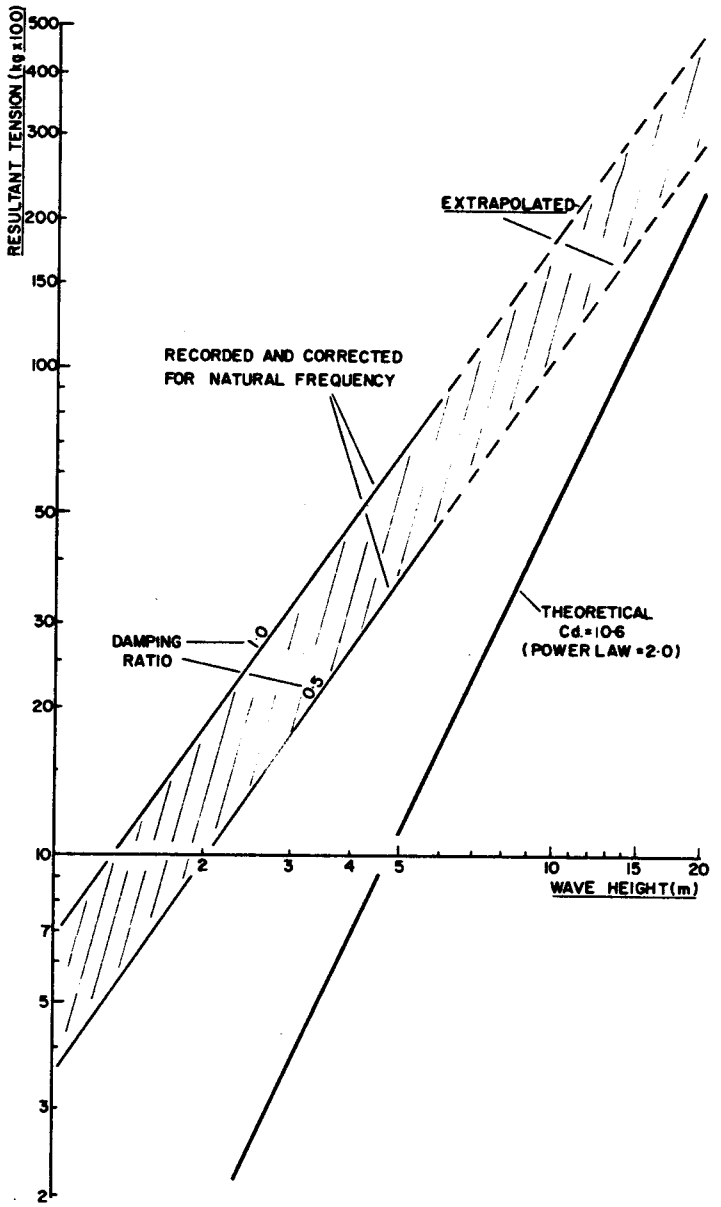

FIGURE 34: Comparison Between the Corrected Wire Tension/ Wave Height Relationship and that Theoretically Predicted

anemometer, aerovane anemometer and transmit and receive antennas. Due to the failure of the base section and the severity of the conditions during the winter months, no attempt was made to reinstall it; and on January 24, 1971, it was towed back to the Bedford Institute. During its time *in situ* 16 system tests and 17 data runs were recorded, and the information obtained is summarized in Table 3. The last recorded information was obtained on December 21 after which the data recording station at Osborne Head was inaccessible due to a heavy snowfall accompanying the storm that caused failure. As no recordings were made during the storm, the exact time or conditions at failure are unknown, but a wave recorder moored in the vicinity during the storm recorded a wave 13 metres high, 10-second period, on December 24, 1970.

Table 4 shows that of the 26 possible comparisons between the forecast wave direction and the direction estimated using the mooring wire tensions agreement was better than 45 degrees in 10 cases and better than 90 degrees in 19 cases. In four of the remaining 7 cases (system tests 2, 3 and 9, data run 13) only 3 of the 4 wire tensions were available; and it is probable that, had the fourth tension been available, agreement would have been better than 90 degrees. Comparing the measured wave height and the forecast wave height shows the maximum overestimate of the wave height was 42% and the maximum underestimate 119%. The over-all trend was to underestimate the wave height by approximately 34%; and of 17 cases where comparison was possible, 13 were underestimated.

Figure 34, the acceleration diagram, shows that the structure oscillated in a north/south direction, regardless of wave direction, which indicates that the natural frequency in pitch in the north/south direction was close to that of the wave loading frequency. The tendency to oscillate more readily in one direction than another was the result of the unsymmetrical layout of the anchors, which produced a higher natural pitch frequency in the north/south direction than in the east/west. The best indicator of the natural frequency in the north/south direction was system test 10 where relatively large horizontal and vertical accelerations were recorded in response to small waves with a frequency of 0.106 Hz. The symmetry of the horizontal acceleration diagram for this test also indicated that the structure was oscillating at its natural frequency. In four of the nine system tests, the maximum acceleration fell between 1.41 and 1.45 m/s^2, and occurred when the structure was moving south during a north/south oscillation. On three of these occasions (system tests 10, 12 and 13), the estimated direction of wave propagation had a southerly (from the south) component and had the four tension recordings been available to estimate the direction on the fourth occasion (system test 2), it would probably have had a southerly component. This suggests that the maximum acceleration occurred as the structure returned from its maximum northerly excursion as a consequence of the combined spring effect in the stretched seaward mooring wires and the drag force caused by the horizontal fluid particle velocity beneath the wave trough. The horizontal particle velocity and, therefore, the direction of action of the drag force beneath the wave trough is opposite to the direction of wave propagation. Although the size of the drag force is greater as the crest passes the structure, it is in opposition to the elasticity in the mooring wires and, consequently, the resultant acceleration is diminished. The magnitude of the maximum resultant horizontal acceleration was independent of the wave height suggesting that the maximum acceleration occurred as the catenary in the

shoreward mooring wires was being removed. The average amount of twist in the structure's motion, as indicated by the change in direction of the resultant acceleration, was 9.6 degrees. This value was supported by the change in direction of the resultant tension (Fig. 31 and 32) which had an average value of 8.5°. As the structure cannot move vertically the presence of vertical accelerations is attributed to 'whipping' of the radio mast and structure, possible misalignment of the accelerometer axes, and the second order effect resulting from the structure's rotation about its base. A one-degree misalignment due to either whipping or misalignment would contribute ±0.0175 x Horizontal Acceleration to the vertical acceleration; and although accelerations due to misalignment would be out of phase with those due to rotation there would be some increase in the maximum value due to the combination of the two effects. Analysis of the acceleration frequency spectra summarized in Table 3 show that both the horizontal components tend to exhibit signs of the natural pitch frequency (0.106 Hz). In addition, horizontal accelerometer channel 10 indicated signs of a second natural frequency at 6.17 Hz, and channel 11 a second natural frequency at 4.62 Hz. Channel 12, the vertical accelerometer channel showed signs of a natural frequency at 8.22 Hz which corresponds to motion in the horizontal direction at 4.11 Hz. The regular occurrence and close proximity of these frequencies suggests that these frequencies were close to the natural frequency of transverse vibration of the structure.

Figure 33, the graph of resultant tension (wave loading) versus wave height using all the available system test and data run information, indicated the following relationship:

$$\text{Resultant Tension (kg x 100)} = 1.8\ (\text{wave height m})^{1.6} \text{ or}$$

$$\text{Wave Loading (kg x 100)} = 1.8\ (\text{wave height m})^{1.6} \cos 22°.$$

Unfortunately, much of the system test and data run information was subject to severe limitations as shown by the key and Figure 36a using only the more reliable data indicated the following relationship:

$$\text{Resultant Tension (kg x 100)} = 3.24\ (\text{wave height m})^{1.26}$$

$$\text{Wave loading (kg x 100)} = 3.24\ (\text{wave height m})^{1.26} \cos 22°.$$

Examination of these two relationships shows that the agreement between the theoretical power law relationship (2.0) and that indicated by the recorded data diminished when only the more reliable data was used. This apparent anomaly is attributed to the lack of reliable data at the higher wave conditions.

Figure 36b uses the same data as Figure 36a and shows the results of an investigation into the possible effect on the data of the structure's natural frequency in pitch. The natural frequency was assumed to be 0.106 Hz as indicated by System Test 10 and as the damping ratio was unknown various values (0.2 to 2.0) were investigated to determine which produced the best straight line relationship. The correlation coefficient attained a maximum value at a damping ratio of 1.0 but remained very close to that value over the range 0.5 to 2.0, suggesting that the actual value of damping ratio could fall anywhere within that range. However, as the associated power law

relationship was moving away from that predicted by the theory at ratios above 1.0, and these higher ratios imply far higher drag coefficients than experiment (Myers *et al.*, 1969) has indicated the actual damping ratio was most probably between 0.5 and 1.0. The correction for natural frequency did improve the agreement between the theoretical and indicated power law relationship.

Figure 37 the comparison between the corrected resultant wire tension/wave height relationship and the theoretical loading calculated using a drag coefficient of 0.6 indicates that the wave loading was underestimated.

9. SUMMARY AND CONCLUSIONS

The placement of the anchor layout for the Mark III was only partially successful as during the first attempt to tension the connecting chain between the concrete anchors the shackle between the mooring wire and the tug's towline failed and the mooring wire was lost. After much difficulty, it was recovered by divers but was extremely difficult to handle as a result of the high stresses placed in it by the towing operation. Consequently, three of the four connecting chains were untensioned and the installation was susceptible to movement of the forward anchors. The recorded tension data showed no evidence of movement, but it may have been a contributing factor in the failure of the mooring system. An investigation to establish whether the anchors did move is in progress, and the results will be reported at a later date. Concrete anchors of the type used are an inefficient form of anchor as their holding power is only 50-60% of their weight in air and some form of screw type anchor with a high reserve of holding power would be more appropriate. Unfortunately, this type of anchor is expensive to install and cannot be re-used.

The cause of failure of the Mark III installation was underestimation of the conditions at the location. This was confirmed by a wave recorder in the vicinity which recorded a 13-metre wave, 2 metres in excess of the design wave, during the storm that caused failure. A wave climate study conducted by Neu (1971) has estimated the 100-year wave off the Nova Scotia coast at 20 metres, and this value should be used in the design of future installations. The immediate cause of failure, wire breakage, could have been prevented by using larger diameter mooring wires; but at the design stage, this did not appear advantageous as the breaking strength of the wire used was already above the holding power of the anchor system. Experience has shown there is some merit in using oversize wires as there is a built-in allowance for corrosion and possible damage during the installation. On the other hand, using oversized wire greatly increases the handling difficulties and, in the final analysis,wire failure is preferable to destruction of the structure. After failure the structure floated with the work platform above sea level and survived at least one severe storm in this condition. The loss of the radio mast and the equipment mounted on it during the storm can be attributed to underdesign of the radio mast guy wire attachment points. An improved design would correct this problem and ensure the equipment was recoverable in the event of a mooring system failure.

During the 2½ months that the Mark III remained in position its performance was monitored in an attempt to check the design calculations. However, while the theoretical loading considered wave loading only, the recorded loading was a measure of the combined effects of wave, current, and wind loading, although due to the limited number and duration of the tests, it is unlikely that any test represented the extreme condition of the maximum wave, maximum wind and maximum current present during any test acting simultaneously. An attempt to correlate the magnitudes of the recorded loadings with the tidal cycle was unsuccessful but tidal currents, ocean current and wind loading obviously contribute to scatter in the data. The recorded data was also modified by the effect of the structure's natural frequency in pitch, which both the design calculations and the recorded data indicate to be within the frequency of wave loading. An attempt to correct for this effect was only partially successful as although it indicated a load/wave height relationship closer to the theoretical and reduced the scatter in the data the damping ratio associated with the structure's motion through the water could not be accurately determined. However, the data does indicate that the damping ratio was sufficient to prevent the frequency of wave loading causing destructive resonance. Other limitations of the recorded data are the necessity to extrapolate over a wide range to reach the design conditions and the conditions at failure, and the limited number of reliable data points.

Accepting these limitations, the comparison between the theoretical and recorded loadings, Figure 37, indicates that the use of a design drag coefficient Cd = 0.6 resulted in an underestimate of the wave loading. Due to the difference in the power law between the theoretical load/wave height relationship and that obtained from the recorded data substitution of a larger design drag coefficient does not result in a better overall agreement. Consequently, should a new stable platform be envisaged one approach would be to carry out the design calculations using the existing theory and a value of drag coefficient that produced agreement with the recorded loading at the design condition. An alternative method would be to modify the theoretical relationship so that it agreed with the recorded data but this possibly attaches too great a value to the limited amount of recorded data. The success of either approach is dependent on the similarity of the new structure to the Mark III and any departure from the basic configuration should be carefully investigated. Having established the design loading a safety factor of at least x2 is recommended. A higher safety factor, x5, would be desirable but the practical difficulty and expense in achieving this value is probably too great.

Although the Mark III failed to withstand the conditions at the entrance to Halifax Harbour, it demonstrated that it would be adequate in a location where the maximum wave height did not exceed 9 metres. From the experience with the Mark III it appears that a structure of this type is feasible, and if the structure and mooring were redesigned, it would be capable of all-weather operation.

10. DESIGN CALCULATIONS

10.1 Introduction

The area that the structure presents to the waves is calculated ignoring any shielding effects and is shown in Figure 38. The magnitude of the wave loading acting on this representative area is calculated using the Morison equation and the second order wave theory for deep water (Section 4, Design). Based on these two relationships the maximum wave loading occurs when the horizontal particle velocity beneath the wave is a maximum which corresponds to the wave crest reaching the structure. Its magnitude for a structure of constant diameter D is given by

$$\text{Maximum loading } F = 1/2\ \rho\ Cd\ D \left(\frac{\pi H}{T}\right)^2 \frac{1}{2k} \left[e^{2kz}\right]_{z=-d}^{z=-\eta_0} \qquad (3)$$

F = total wave force (N)

ρ = mass density (kgm/m^3)

Cd = drag coefficient

D = representative diameter (m)

H = wave height (m)

T = wave period (sec)

k = wave number = $2\pi/L$ (m^{-1})

z = position relative to mean water level (m)

η_0 = wave crest height above mean water level (m)

$$\frac{\eta_0}{H} = \tfrac{1}{2} + \tfrac{1}{4}\left(\frac{\pi H}{L}\right)^2$$

d = structure length below mean water level (m)

The point of action of the wave loading $\bar{z}$, relative to the mean water position is given by

$$\bar{z} = \left[e^{2kz}\left(z-\frac{1}{2k}\right)\right]_{-d}^{\eta_0} \Big/ \left[e^{2kz}\right]_{-d}^{\eta_0} \qquad (4)$$

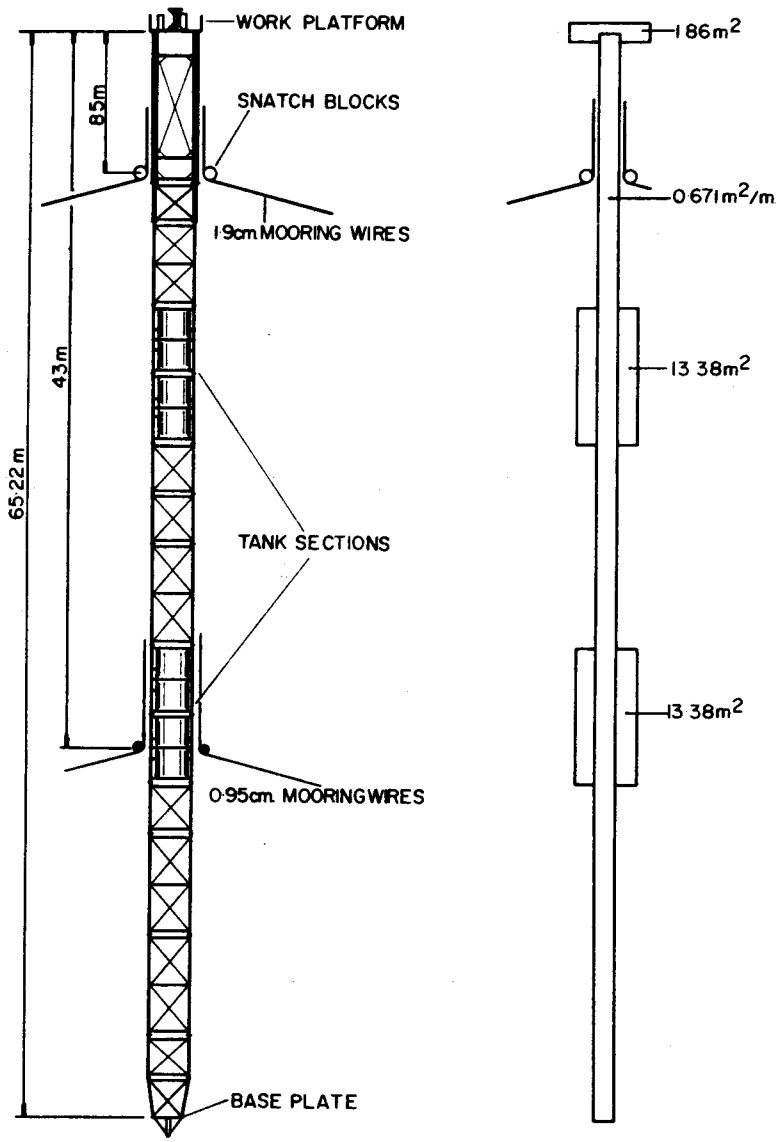

FIGURE 38: Area Representation

Equations 3 and 4 are only applicable to the uniform area running the length of the structure and the loadings on the tank sections and work platform are treated as point loads of magnitude dependent on the horizontal particle velocity at their mean position.

The calculation of wave loading using the method described is subject to several limitations including the validity of the Morison equation and the second order wave theory for deep water and the method of representing the structure for wave loading calculations.

10.2 Wave Loading for Design Wave Height 11 metres, Period 12 seconds

Load on 0.671 m^2/m area running length of structure.

$$\text{Load} = \tfrac{1}{2}\,\rho\,Cd\,D\left(\frac{\pi H}{T}\right)^2\frac{1}{2k}\left[e^{2kz}\right]_{z=-d}^{z=\eta_0}$$

$\rho = 1035$ kgm/m^3, $Cd = 0.6$

$D = 0.671\ m^2/m$, $L = 1.56T^2 = 224.6$ m,

$K = 2\pi/L = 0.0280$, $H = 11$ m, $d = 58.82$ m

$$\frac{\eta_0}{H} = \tfrac{1}{2} + \tfrac{1}{4}\left(\frac{\pi H}{L}\right)^2 \qquad \eta_0 = 5.56 \text{ m}$$

$$\left(\frac{\pi H}{T}\right)^2 = 8.295$$

$$= 40{,}983.64 \text{ N}$$

$$= \underline{4{,}177.74 \text{ kgf}}$$

$$\bar{z}\left[e^{2kz}\right]_{z=-d}^{z=\eta_0} = \left[e^{2kz}\left(z - \frac{1}{2k}\right)\right]_{z=-d}^{z=\eta_0}$$

$\underline{\bar{z} = 10.51 \text{ m}}$

Load on upper tank section, position z = -14.02 metres.

Load = ½ ρ Cd A V

ρ = 1035 kg/m^3, Cd = 0.6

A = 13.38 m^2, $V^2 = \left(\frac{\pi H}{T}\right)^2 e^{2kz} = 3.788$

= 15,737.21 N

= <u>1604.2 kgf</u>

Load on lower tank sections, position z = -34.44 metres.

Load = ½ ρ Cd A V

ρ = 1035 kgm/m^3, Cd = 0.6, A = 13.38 m^2

$V^2 = \left(\frac{\pi H}{T}\right)^2 e^{2kz} = 1.202$

= 0.5x1035x13.38x0.6x1.202

= 4994.42 N

= <u>509.11 kgf</u>

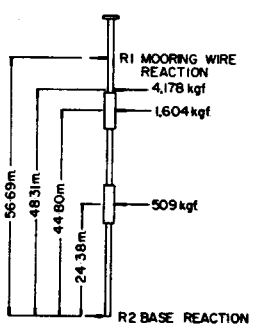

$R_1 + R_2 = 6291.05$ kgf

$R_1 = 5046.87$ kgf $\qquad R_2 = 1244.18$ kgf

Figure 39 shows the shear force and bending moment diagrams under this system of loading.

10.3 Determination of Safety Factors

Structure

'I', second moment of area, for structure

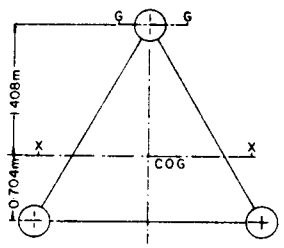

Igg for each leg = 4×10^{-6} m^4

Area of each leg = 0.00284 m^2

h = distance from C.O.G.

$$Ixx = Igg + Ah^2$$

$$= 3x4x10^{-6}+(1.408)^2x0.00284+2x0.704^2x0.00284$$

$$= \underline{0.008457\ m^4}$$

$$\text{Maximum stress} = \frac{M}{I} ymax$$

M = maximum bending moment, see Figure 39

ymax = maximum distance from C.O.G. = 1.408 m

$$\text{Maximum stress} = \frac{30.5x10^3x1.408}{0.008457}$$

$$= \underline{5078\ tonf/m^2}$$

Yield stress = $\underline{21{,}090\ tonf/m^2}$

∴ $\underline{\text{Safety factor} = 3:1}$

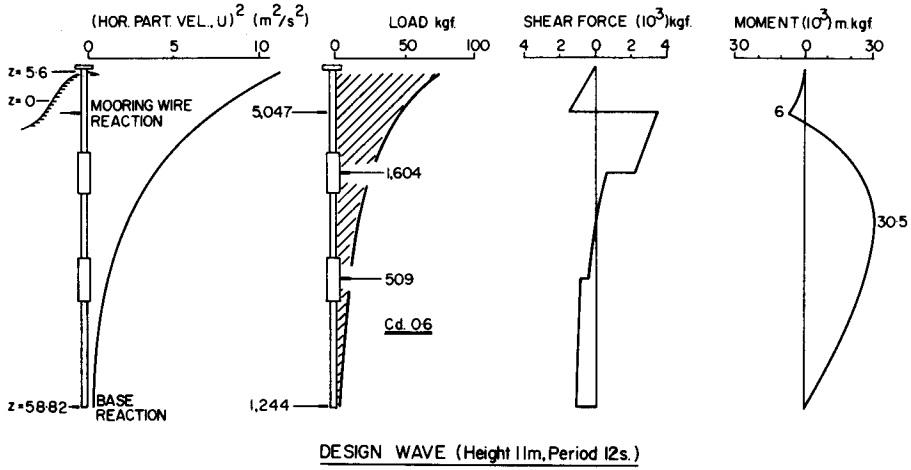

FIGURE 39: Load, Shear Force and Bending Moment Diagram

Mooring Wires

Breaking strain of 1.9 cm diameter, 6x24 wire = 16,800 kgf

If all load taken by one wire load = 5047/cos 22 = 5460 kgf

. . Safety Factor = 3:1

Anchor Holding Power

Maximum horizontal load on one anchor = 5047 kgf

Holding power of anchor = 11,400 kgf

. . Safety factor = 2:1

10.4 Structure Movement under Wave Loading and Resulting Accelerations

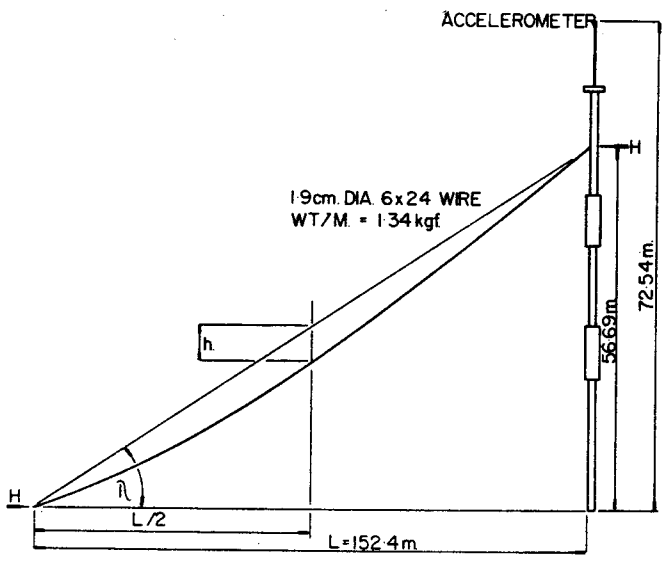

The total movement of the structure at the mooring wire attachment point consists of catenary movement (Norris and Wilbur, 1960) and elastic stretch of the mooring wires. The catenary movement is dependent on the load and amount of pretensioning and the elastic stretch on the load only.

Catenary Movement

$H = \frac{wL^2}{8h}$ where H, horizontal force (kgf)

L, horizontal distance between anchor and structure (m)

w, weight/metre of wire (kgf/m)

h, mid-point sag (m)

$x = \frac{8L\theta^2}{3 \sec^2 \lambda}$ where x, difference between chord length and catenary length between anchor point and structure (m)

$\theta = h/L$, sag ratio

λ , chord angle, 22 degrees

Elastic Movement

$e = \frac{L\ Tav}{E\ A}$ where e, stretch (m)

L, wire length (m)

Tav, average wire tension = $H \cos\lambda$ (kgf)

E, Young's Modulus, 7030×10^6 (kgf/m^2)

A, csa of wire = 0.6 nominal area (m^2)= 0.00017 m^2

Table of sag h, sag ratio θ, Tav, x and e for various values of H

H(kgf)	h (m)	θ	Tav (kgf)	x (m)	e (m)
750	5.19	0.0341	809	0.377	0.103
2,500	1.56	0.0102	2,696	0.0337	0.344
5,000	0.78	0.0051	5,393	0.0084	0.688
10,000	0.39	0.0026	10,785	0.0022	1.375

If the mooring wires are pretensioned to 750 kgf the following movements will take place:

H (kgf)	Elastic Stretch (m)	Catenary (m)	Elastic + Catenary, z (m)
2,500	0.241	0.343	0.584
5,000	0.585	0.369	0.954
10,000	1.272	0.375	1.647

The purpose of the structure is to provide a stable mounting point for the thrust anemometer on the top of the radio mast and therefore the motion at this point is of particular interest. If the flexural motion of the structure is assumed to be negligible the movements at the mast top under the various loadings are

H (kgf)	Wire Movement z (m)	Horizontal Movement, z cos 22° at wire attachment point (m)	Horizontal Movement, A, at mast top z cos 22x72.54/56.69 (m)
2,500	0.584	0.451	0.692
5,000	0.954	0.885	1.132
10,000	1.647	1.527	1.954

If the assumption is made that the horizontal movement varies sinusoidally at the frequency of wave loading the maximum acceleration can be estimated from

Displacement = A sin ωt where A = horizontal movement

ω = wave frequency rad/s

Acceleration = A ω^2 sin ωt

The acceleration is maximum when sin ωt = 1, and can be estimated for various values of ω in association with various wave loadings.

Wave Period T (s)	Loading Frequency $\omega = \frac{2\pi}{T}$ (rad/s)	Loading H (kgf)	Horizontal Movement A (m)	Acceleration = A ω^2 (m/s^2)
6	1.04	2,500	0.692	0.75
6	1.04	5,000	1.132	1.22
6	1.04	10,000	1.954	2.11
10	0.63	2,500	0.692	0.28
10	0.63	5,000	1.132	0.45
10	0.63	10,000	1.954	0.76

The accelerations given in the above table are calculated using the assumption that the mooring wires are in the same plane as the structure's motion. This is not the case and due to the unsymmetrical layout of the anchor system the movement, and therefore the resulting acceleration, is dependent on the direction of loading. For a loading direction midway between the 60 degree included angles of the anchor layout the accelerations above should be multiplied by 1.16, and by 2 for a loading direction midway between the 120 degree included angles.

10.5 Response to Wave Forces

Heave Response. As the total weight of the structure with the lower tanks flooded exceeds the uplift forces under all conditions the heave response will be zero.

Pitch Response. The pitch response can be approximated to the motion of a single degree of freedom system with forced oscillation (Pearlman, 1964) the natural frequency of which is given by

$$f = \frac{1}{2\pi}\sqrt{\frac{F}{M}}$$ where f = natural frequency (Hz)

F = system stiffness (m N/rad)

M = system mass movement of inertia ($kgm\ m^2$)

To simplify the calculation of the mass moment of inertia it is assumed that the mass of the structure is concentrated at its mid-point and that of the fluid in the lower tanks at the tank centre. The added water mass, which for a cylinder in horizontal motion is equal to the mass of the fluid displaced (Lystrad and Stromme, 1970) is also assumed to be concentrated at

the tank centres. The effect of added water mass on the structural members is ignored.

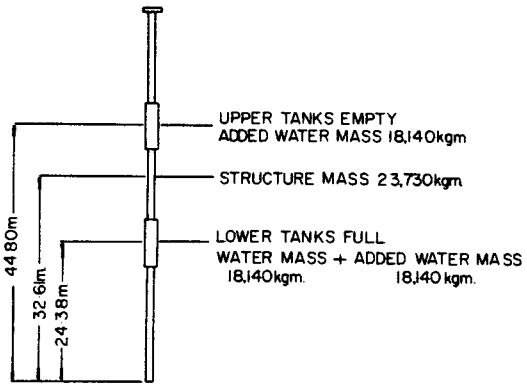

Mass moment of inertia M = mass moment inertia of structure + mass moment inertia of fluid in lower tank + mass moment of inertia of added water mass of upper and lower tanks.

$M = 23,700 \times 32.61^2 + 18,140 \times 44.8^2 + 18,140 \times 24.38^2 + 18,140 \times 24.38^2$

$= 8321 \times 10^4$ kgm m^2

The system stiffness in pitch motion is given by the summation of the restoring forces provided by the guy wires and the upper buoyancy tanks. For very small angles the restoring moment due to buoyancy can be neglected and the restoring moment assumed to be dependent on the guy wire stiffness only. The guy wire stiffness, dependent on the elastic nature of the wire and the catenary movement, is determined using the information on horizontal movement derived in part 4 of the design calculations.

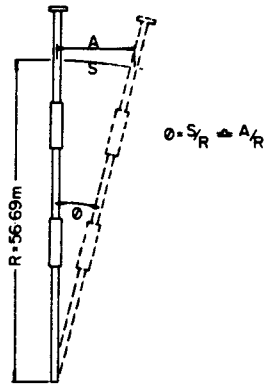

Load H(kgf)	Movement A (m)	Angular Movement θ (rad)	Angular Stiffness H/θ (N/rad)	Restoring Moment Stiffness F=HR/θ (m N/rad)	Natural Frequency $= \frac{1}{2\pi}\sqrt{\frac{F}{M}}$ Hz
2,500	0.541	0.0095	258×10^4	146×10^6	0.21
5,000	0.885	0.0156	314×10^4	178×10^6	0.23
10,000	1.527	0.0269	365×10^4	207×10^6	0.25

If the movement is corrected to allow for the actual anchor layout, that is, x1.16 for loading midway between 60 degrees included angle and x2 for 120 degrees included angle we have,

Load (kgf)	Restoring Moment Stiffness for 60°	Restoring Moment Stiffness for 120°	Natural Frequency 60°	Natural Frequency 120°
2,500	126x10	73x10	0.19	0.15
5,000	153x10	89x10	0.22	0.16
10,000	178x10	104x10	0.23	0.18

From the above calculations it appears that the natural frequencies present in the structure will vary between 0.15 Hz (period 6.7 s) to 0.25 Hz (period 4 s).

10.6 Natural Frequency of Transverse Vibration of Structure

Due to the elastic nature of the structure a small natural flexural vibration may occur if a bending force is exerted, the frequency being dependent on the flexural stiffness and mass distribution of the structure. In the moored position the lower tanks are flooded which results in an increase in the structure mass. For transverse vibration in water the mass is further increased by an added water mass which for a cylinder in horizontal motion is equal to the mass of fluid displaced. The resulting mass distribution is shown.

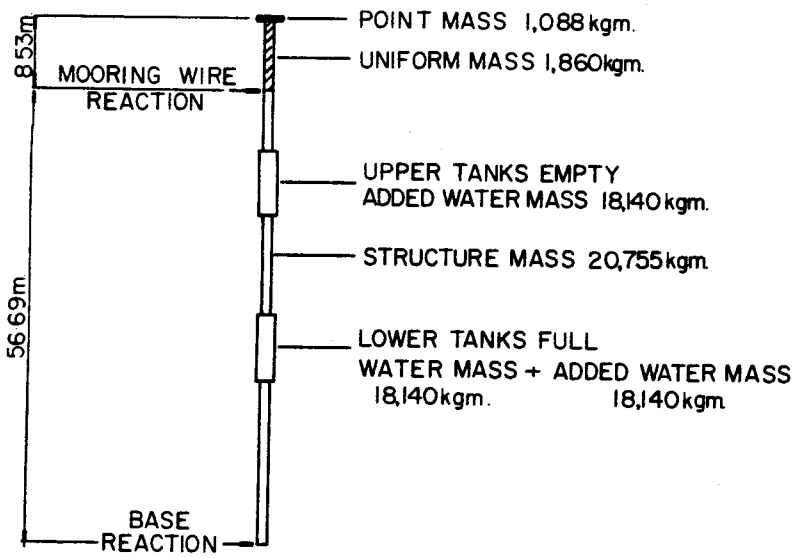

Because of the inhomogenity of the mass distribution and the variation in damping forces along the axis it is difficult to predict the pattern of the bending oscillations. To simplify the calculations two different modes of oscillation are considered and the resultant oscillation assumed to fall between the two extremes (Hamer, Lystad and Stromme, 1970).

First Mode. To determine the natural frequency in the first mode the effect of the 8.5 metre cantilevered top section is ignored and the structure considered to be a simply supported beam with its total mass, including the added water mass, uniformly distributed over its length.

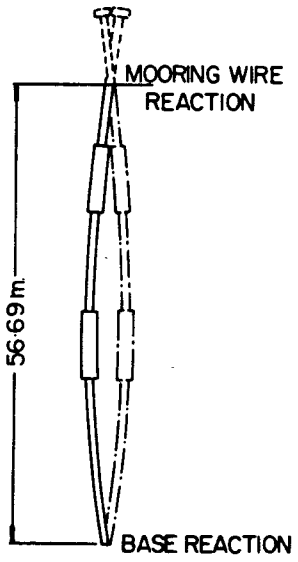

Natural frequency in this mode
(Roark, 1965)

$$f = \frac{0.626}{\sqrt{\frac{5}{384}\frac{MTL^3}{EI}}}$$

E Young's modulus = $21,090 \times 10^6$ kgm/m^2

MT Total mass (including added water mass) = 75,175 kgm

I Inertia = 0.008457 m^4

L Length = 56.69

$f_1 = 0.626$ Hz

Second Mode. The second mode considers the 56.69 of structure beneath sea level as stationary and assumes that only the cantilevered portion oscillates. The cantilevered portion is assumed to consist of a uniformly distributed mass with a point-mass at the end.

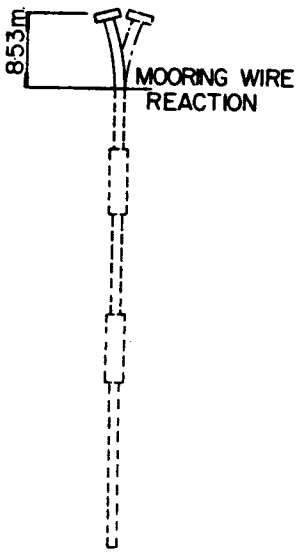

Natural frequency of this mode
(Roark, 1965)

$$f = \frac{0.552}{\sqrt{\frac{(m_1+0.236\ m_2)L^3}{3EI}}}$$

E Young's modulus = $21{,}090 \times 10^6$ kgm/m^2

I Inertia = 0.016914 m^4

m_1 Point mass = 1088 kgm

m_2 Uniform mass = 1860 kgm

L Length = 8.53 m

f_2 = 18.6 Hz

The natural frequencies of transverse vibration of the overall structure are thus considered to fall between 0.63 Hz and 18.6 Hz which is outside the frequency spectrum containing significant wave energy. Due to the far reaching assumptions made in these calculations these frequencies can only serve as a crude indicator to the actual frequencies.

11. ACKNOWLEDGEMENTS

The most difficult part of this project was the installation of the structure as described in Section 5. The concrete anchors, the floating crane and the personnel used to place the anchors were supplied by the Department of National Defence at the request of AOL. The tug used to tow the floating crane during the placing of the anchors and the structure during the mooring operation was supplied by Foundation Maritime, Halifax, N.S. The fishing boat used in both parts of the installation was the Fisheries Research Board vessel *Sigma-T* and the diving services required during the mooring operation were provided under contract by Maritime Divers, Dartmouth, N.S. The extensive knowledge of the ocean required to devise a method for mooring a structure of this type was provided by Mr. G. Henneberry of Sambro, N.S., and I would like to express my sincere thanks for his invaluable assistance. I would also like to acknowledge the assistance ofJ. Brooke, C.S. Mason, S.D. Smith, S.B. MacPhee and D.F. Dinn in the preparation of this report.

12. REFERENCES

BENDELL, E.A. 1970. Turbulence Thermistor Manual. Atlantic Oceanographic Laboratory File No. 5420-10.

DEANE, R.E. 1963. Limnological and Meteorological Observation Towers in the Great Lakes. *Limnology and Oceanography, 8.*

DINN, D. 1972. A Remote-Controlled, Multi-Channel, Analog-Data, Telemetry System. Atlantic Oceanographic Laboratory, Bedford Institute, N.S., Canada. Report in preparation.

DOBSON, F.W., and R.F. BROWN. 1972. A Set of Programs for Analysis of Time Series Including Fast Transform Spectral Analysis. AOL report in preparation.

DOE, L.A.E. 1963. A Three-Component Thrust Anemometer for Studies of Vertical Transport above the Sea Surface. AOL Report BI 63-1, 87 pp.

DOE, L.A.E., and J. BROOKE. 1965. A Moored Stable Platform for Air-Sea Interaction Studies. *Limnology and Oceanography, 10.*

GIBB, ALBERY, PULLERITS and DICKSON. 1969. Air Sea Interaction Study Platform. AOL File No. 5020-10.

HAMER, LYSTAD and STROMME. 1970. Open Ocean Manned Observation Platform, A Preliminary Investigation of Design and Dynamic Positioning. Chr. Michelsens Institute, Department of Applied Physics, Bergen, Norway. Ref. CMI No. 69059-1/0D, 99 pp.

HOGBEN, N., and F.E. LUMB. 1967. Ocean Wave Statistics. Her Majesty's Stationery Office.

LYSTAD, L.P., and J. STROMME. 1970. Unmanned Open Ocean Observation Platform, A Preliminary Investigation of Design and Positioning. Chr. Michelsens Institute, Dept. of Applied Physics, Bergen, Norway. Ref. CMI No. 70010-1/LPL/JS, 54 pp.

MORISON, J.R., M.P. O'BRIEN, J.W. JOHNSON, and S.A. SCHAAF. 1950. The Force Exerted by Surface Waves on Piles. *Petroleum Transactions, AIME, (1950), 189.*

MYERS, HOLM and McALLISTER. 1969. Handbook of Ocean and Underwater Engineering. McGraw Hill, Chapter 12, p. 51.

NEU, H.A. 1971. Wave Climate Study of the Canadian Atlantic Coast and Continental Shelf - 1970. AOL Report 1971-10, 175 pp.

NORRIS and WILBUR. 1960. Elementary Structural Analysis, Chapter 10, Cables. McGraw Hill, pp. 276-285.

PEARLMAN, M.D. 1964. Considerations for the Optimization of Particular Characteristics of Stable Buoys. *Transactions of the Buoy Technology Society*, pp. 17-29.

PETERSON, P.L., R.T. MAELSIG, and D.K. FORSEEN. 1969. Structural Design of an Instrumented Mast to be Emplaced on Cobb Seamount in the Northeastern Pacific Ocean. Offshore Technology Conference, Paper No. OTC 1060, 1969, pp. I-647 - I-648.

ROARK, R.V. 1965. Formulas for Stress and Strain, Chapter 15, Dynamic and Temperature Stresses. McGraw Hill, p. 369.

SMITH, S.D. 1969. A Sensor System for Wind Stress Measurement. Atlantic Oceanographic Laboratory, Bedford Institute, N.S., Canada. Report BI 1969-4, 64 pp.

SMITH, S.D. 1970. Thrust Anemometer Measurements of Wind Turbulence, Reynolds Stress, and Drag Coefficient over the Sea. *J. Geophys. Res.*, *75*, pp. 6758-6770.

SMITH, S.D., and R.F. BROWN. 1971. Program A TO D for Analog to Digital Conversion of Time Series Data. AOL Computer Note 1971-2C, 51 pp.

THORBURN, J.P., and D.F. DINN. 1971. On-Line Analog to Digital Hardware at the BI Computing Centre. AOL Report 1971-3, 17 pp.

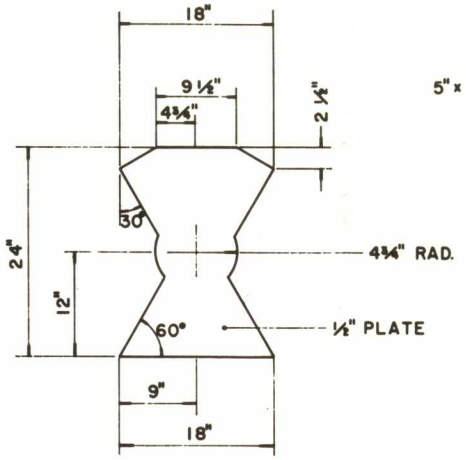

DETAIL OF PAD

SCALE 1:8

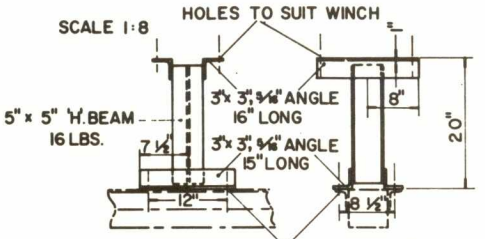

WINCH MOUNTS 4 OFF

5 TON BULLDOG WINCH, MARINE
MODEL BEEBE HM8
MARPOLE MACHINE WORKS LTD.,
1422 SOUTH WEST MARINE DRIVE
VANCOUVER B.C.

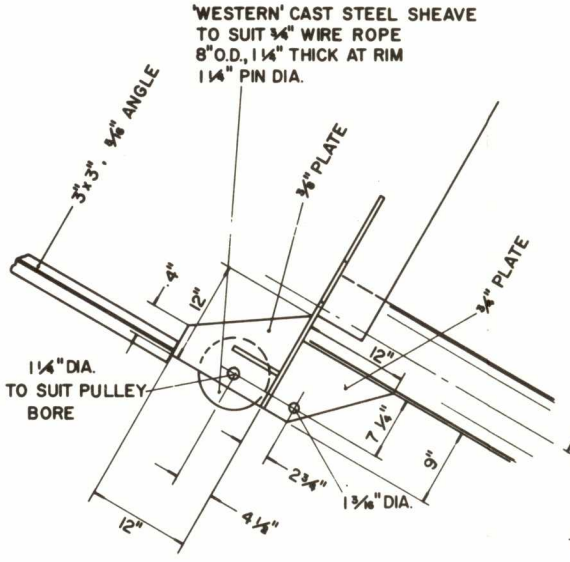

PULLEY BRACKET & CABLE
ANCHOR POINT
TYPICAL OF 4 POSITIONS

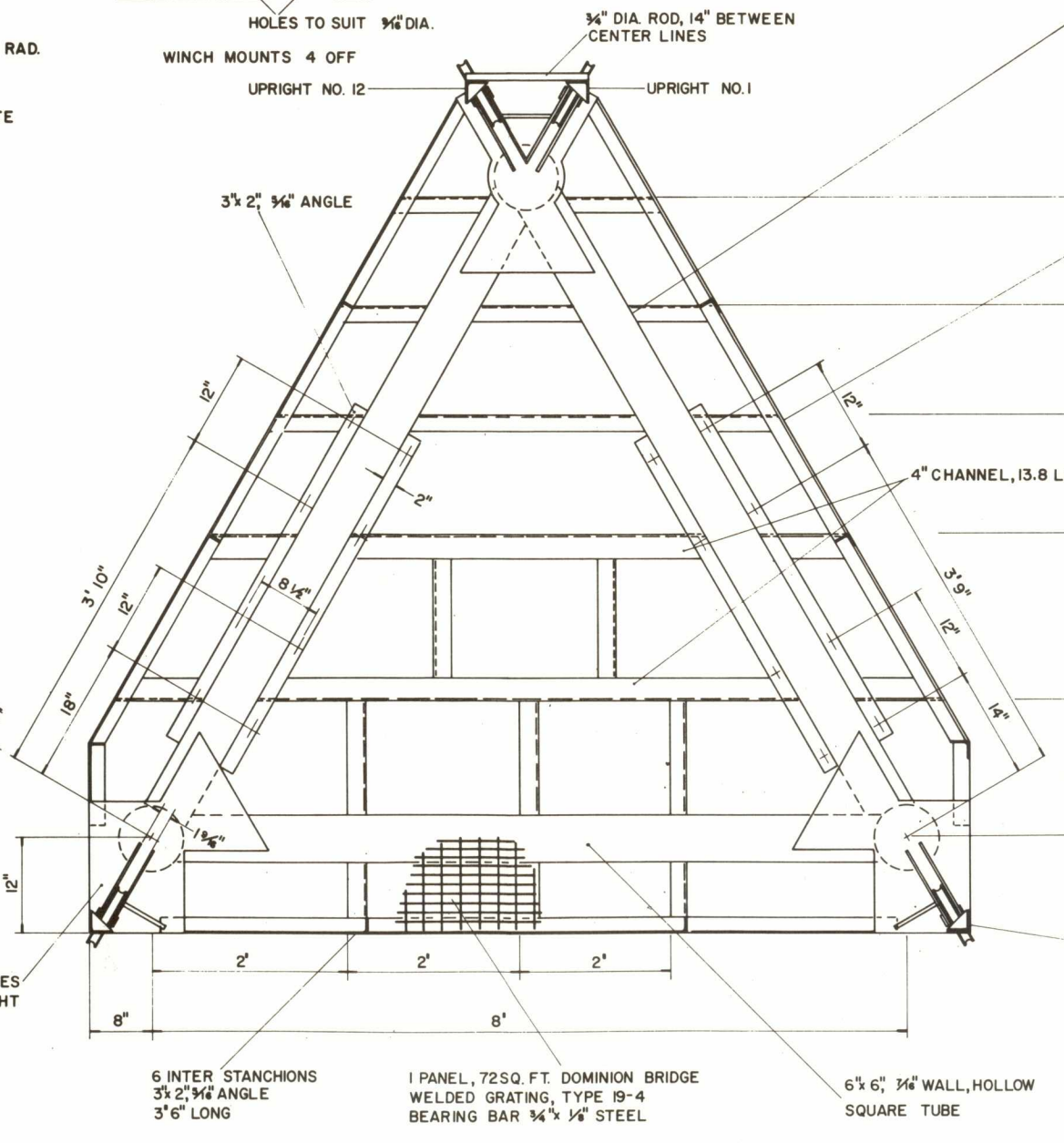

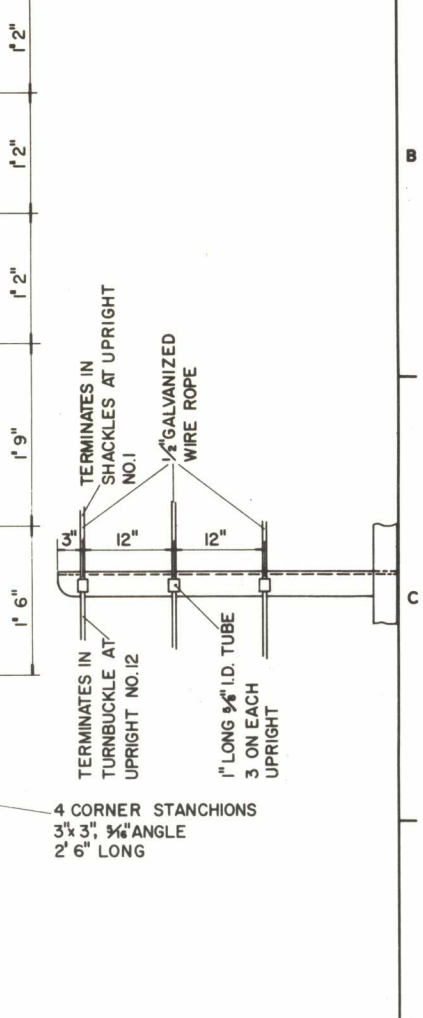

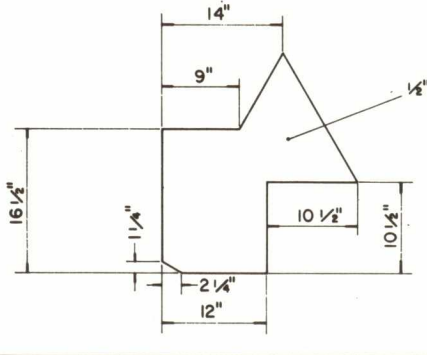

PLATFORM DETAILS

BEDFORD INSTITUTE DARTMOUTH — NOVA SCOTIA	
TITLE: MARK 3 STABLE PLATFORM	
DWN. R. G. MILLS	
DATE 25-4-70	SHT. 2
DRAWING NO. E-B-19-2	

PLATFORM WT. 2,400

218' TOTAL WT. 52,260 lbf INC. FITTINGS 1,320 lbf.

29' 6"	4,100		'A'	UPPER SNATCH BLOCKS
8'	1,130		'B'	
16' 2"	2,000		'C'	
13' 7"	6,600	TANK 4	'D'	
13' 7"	6,900	TANK 3	'E'	
10'	1,300		'F'	
10'	1,300		'G'	
20'	2,200		'H'	
13' 7"	7,200	TANK 2	'I'	
13' 7"	7,200	TANK 1	'J'	LOWER SNATCH BLOCKS
10'	1,300		'K'	
20'	2,200		'L'	
20'	2,200		'M'	
8'	1,100		'N'	
12'	1,810		'O'	

SCALE 1/8" = 1ft

8' TYP.

SECTIONS N, K, G & F

SECTIONS M, L & H

9" 9" 9" 9" 6"

3/4" RODS

2½ SCHD. 40

4" SCHD. 80

3/4" RODS

SCALE 1" = 2FT

3/4" RODS

2½" SCHD. 40

2½" SCHD. 80

1⅛" ROD

9" DIA. 8 HOLE (TYP.)

2½" SCHD. 80

1⅛" ROD

FLANGE ANGLE 4·25

½" THK. 6" DP

4 GUSSETS ⅜" PL

6" SCHD. 80

1'9" 4'6" 2'3" 12"

3'10"

5'9" DIA. ⅜" PL.

5'-2" DIA. P.C.D

1" OVERLAP

4" SCHD 80

1¼" THK. 6'3" DIA. RING

⅜" PLATE

VIEW ON 'A A' TYP. ALL 4 TANKS

1¼" THK. 6'3" DIA. RING TYP. ALL 4 TANKS

ZINC ANODES 6 PER TANK.

4" x 4" x ¼" ANGLE TOP & BOTTOM TYP. ALL 4 TANKS

6" DP ⅜" THK. RINGS 2 PER TANK

4' of ⅜" PL. TYP. 13' 7"

4" SCHD. 80 PIPE. TYP. ALL 4 TANKS.

2" SCHD. 40 WATER OUTLET AT TANK BOTTOM.

1" SCHD. 40 AIR INLET AT TANK TOP. TYP. ALL TANKS.

5" DP. 5/16" THK.

2 PER TANK MANHOLE 1'-8" x 1' 4"

3½" DP. ¼" THK.

2" BRONZE GATE VALVE 1 PER TANK.

9" DIA. 8 HOLE FLANGES

6 OFF EQUI-SPACED 6" x 4" x ⅜ ANGLES

EX. R.C.N. MOORING BUOY. 12' LG. 5'9" DIA. ⅜" THK. TYP. ALL SECN.

TANK No. 1

TANK No. 2

9 OFF EQUI-SPACED 3" x 3" x 5/16" ANGLES

TANK No. 3

9 OFF EQUI-SPACED 2" x 3" x ¼" ANGLES

TANK No. 4

SEE SHT. 2 FOR PLAT. DET.

6" x 6" x ⅜" HOLLOW SQUARE TUBE

18" 4" SCHD. 80

½" THK. D'BLR PLATES

1" DIA 12" GALV. T'BUCKLES

¾" WIRE

8" SCHD. 40

4" SCHD. 80

WIRE CLIPS

4" SCHD. 80

SECTION A

5' 18" 18" 29' 6" 5' 8" 2' 6'8" 8"

13½" DIA. 8 HOLE FLANGE

1½" DIA. ¾" THK. PLATE

9"R 120° 6" 2½" ½" PLATE

BACK LEG

R.H. FRONT LEG

SHEAVE MOUNTING DETLS.

⅜" DIA. VERT'S WHOLE LENGTH

4" 12"

8" SCH 80 3"

RUNG DET'S

20 RUNGS. ¾" DIA. BAR 14" BETWEEN EA. RUNG ALL 3 LEGS.

SHEAVE MOUNTINGS TO SUIT McKISSICK LIGHT TYPE CHAMPION SNATCH BLOCKS TYPE 419, WITH SHACKLE, SHEAVE 8", WIRE ¾", BRONZE BUSHING, S.W.L 15 TONS. 4 OFF. ALSO 4 OFF WITH 6" SHEAVE FOR FITTING TO TANK 'I'. SIMILAR TO ABOVE.

1' 3" SCHD. 40 2" SCHD. 40 6" SCHD. 80 3" SCHD. 40 2½" SCHD. 40 1" DIA. 4" SCHD. 80 8' 16' 2"

11" DIA. 8 HOLE FLANGES

REMOVABLE QUICK DISCONNECT COUPLINGS ¾

1" & 2" MARINE BRONZE GATE VALVES CRANE NO. 1, 125 P.S.I., GLOBE & ANGLE.

ALL PIPES TERMINATE AT THIS LEVEL.

SECTIONS B & C

PAINT SYSTEM

TOP 40'

I. COMMERCIAL BLAST NO. 6
II. MOBIL INORGANIC ZINC NO. 7, 1 COAT 3 MIL
III. MOBIL SOCOPOL VINYL ENAMEL 69-R-9, RED, 2 COATS 1·5 MIL THK. EA.

REMAINING 178'

I. COMMERCIAL BLAST NO. 6
II. INORGANIC ZINC AS ABOVE
III. MOBIL ALUMINUM BARRIER COAT 59-A-2 1 COAT 2 MIL
IV. MOBIL ANTIFOULING 1 COAT 3 MIL 59-D-1

BEDFORD INSTITUTE
DARTMOUTH —— NOVA SCOTIA

TITLE
MARK 3 STABLE PLATFORM.

DRN. R.S.M.L.S.
DATE 12-5-70

DRAWING NO. E-B-19-1